SPECTROSCOPIC MEASUREMENT OF NITRIC OXIDE IN A DIFFUSION FLAME

by

Dimitris Valougeorgis

Thesis submitted to the Faculty of the
Virginia Polytechnic Institute and State University
in partial fulfillment of the requirements for the degree of

MASTER OF SCIENCE

in

Mechanical Engineering

APPROVED:

D. R. Jaæsma, Chairman

H. L. Wood

G. J. M. Indebetouw

June, 1982

Blacksburg, Virginia

ACKNOWLEDGMENTS

The author is grateful to Dr. Dennis R. Jaasma for his help, guidance, and encouragement throughout this research. Dr. H. L. Wood and Dr. G. M. Indebetouw are thanked for their service on the examining committee. The assistantship provided by the Mechanical Engineering Department was greatly appreciated. Special thanks are extended to the National Science Foundation for funding this work.

The author would also like to thank his wife Jenny for her support throughout his graduate studies and his parents for their encouragement during his academic career.

TABLE OF CONTENTS

TABLE OF CONTENTS (continued)

LIST OF FIGURES

LIST OF FIGURES (continued)

LIST OF FIGURES (continued)

LIST OF TABLES

NOMENCLATURE

$A_{background}$	background absorption, per cent
A_{λ}	per cent spectral absorption at wavelength λ
A_{total}	total absorption
C_{NO}	nitric oxide concentration, ppm
C_{O2}	oxygen concentration, ppm
δ	refractive index minus one
K_{λ}	spectral absorption coefficient at wavelength λ, $(\text{ppm cm})^{-1}$
λ	wavelength, nm
L	length of optical path, cm
n	refractive index
o	reference state, T = 273 K, P = 1 atmosphere
r	radius, m
T	temperature, K
ξ_D	optical line width, nm

I. INTRODUCTION

Nitric oxide and nitrogen dioxide are recognized as major air pollution problems. For that reason, NO and NO_2 formation in combustion systems has been under intensive study by goverments and private research agencies for several years. Basic to these studies is the determination of the chemical reactions which form NO and NO_2.

We are fortunate in having a relatively good understanding of NO formation. Zeldovich's (1) mechanism has been successful in predicting NO formation rates for a wide range of combustion systems. In contrast, our knowledge of NO_2 formation kinetics is very limited.

Several investigators have indicated the presence of NO and NO_2 in flames. The validity of these results has been challenged because it is notoriously difficult to measure the NO_2 concentrations in high temperature gases, since NO is readily converted to NO_2 in the sampling system. It is believed that reactions with flame radicals, which occur when the sample is quenched in the sampling probe, destroy the in-flame concentrations of NO and NO_2.

In view of the current lack of understanding of nitrogen dioxide formation, this work experimentally investigates the formation of NO_2. Recent experiments have given startling data which indicate that the thermal NO produced by a laminar diffusion flame is oxidized to NO_2 if the air around the flame is doped with unburned hydrocarbons (2). It is believed that the breakdown of hydrocarbon species and their subsequent oxidation outside the flame envelope can produce HO_2 and OH, which in

turn could scavenge the NO molecules diffusing out from the peak temperature region where they are formed. Probe sampling could perhaps be used to verify that NO is converted to NO_2 outside the flame, but the issue is clouded by questions concerning NO to NO_2 conversion in probes and sampling systems. Probe reactions such as

$$NO + O \rightarrow NO_2$$

or

$$NO + HO_2 \rightarrow NO_2 + OH$$

could lead to a shift between NO and NO_2 (3). Because optical methods are characterized by not interfering with the easily disturbed flame, it appears that an in-situ measurement of NO using spectroscopic techniques could give information which is not otherwise obtainable.

The objectives of this research are to:

1. Use spectroscopic measurements of NO concentrations in a diffusion flame to confirm or deny the conversion of NO to NO_2 in or near the flame.
2. Provide a comparison between probe and optical NO concentration measurements.

The remainder of the thesis is organized in the following way. Chapter II reviews the literature on NO/NO_2 formation, while Chapters III and IV describe the apparatus and procedures used in the

investigation. The remaining three chapters cover the results, conclusions, and recommendations.

II. LITERATURE REVIEW

Regarding fundamental research, diffusion flames initially received less attention than premixed flames despite the fact that diffusion flames are more common in industry. Part of this neglect has been due to the lack of an easy-to-study, one-dimensional diffusion flame. Also, the mass transfer adds greatly to the complexity of the problem. In this survey, a general review of the previous work on diffusion flames is first given, and then our knowledge of NO and NO_2 formation in both premixed and diffusion flame systems is summarized. Previous workers' attempts to make in-situ NO and NO_2 measurements are described and a discussion of probe errors is also included.

In 1928 Burke and Schumann (4) produced the first simple analytical treatment of a steady diffusion flame structure for a single reaction of infinite rate and showed that the local concentrations of gases could be calculated. This model was modified by Barr (5), who studied the complex structure of the flames of hydrocarbons in vitiated air. Fendell (6,7), Chung and Blankens (8) in 1966, and Clarke (9,10) in 1967 interpreted the original Burke-Schumann flame sheet model as a singular perturbation problem. Clarke (11) extended the model by the method of matched asymptotic expansions for a set of reactions in chemical equilibrium and for systems not in that chemical state (12). The burner configuration was an idealisation of the two-dimensional Wolfhard-Parker burner, and the conservation equations were simplified by the use of the Oseen approximation. Melvin, Moss, and Clarke (13) in

1971 compared their experimental results of the structure of a flat diffusion flame on a Wolfhard-Parker burner with theoretical predictions of solutions which incorporate realistic schemes for the chemical kinetics. Their experiment shows that close to extinction there is a significant convective transfer of material, from one stream to the other, at the flame base. This phenomenon can not occur in a diffusion flame around a porous cylinder or in an opposite jet flame burner, because the reaction zone prevents the premixing of fuel and oxygen molecules.

Current concerns over nitrogen oxide emissions have prompted many investigators to a more detailed examination of the nitrogen oxide formation process in diffusion and premixed flames. Most of these studies have focused primarily on the formation of NO in the postflame gases of premixed flames, where 90-95 per cent of the fixed nitrogen is present as nitric oxide. For the most part, NO formation in postflame gases is explained by the Zeldovich (1) mechanism

$$O + N_2 \rightarrow NO + N \tag{1.1}$$

$$N + O_2 \rightarrow NO + O \tag{1.2}$$

Some studies report NO levels in the visible flame zone greater than can be accounted for by the Zeldovich mechanism. Fenimore (14) labeled this excess NO as "prompt NO" and has suggested that reactions such as

$$CH + N_2 \rightarrow HCN + N \tag{1.3}$$

$$C_2 + N_2 \rightarrow 2CN \qquad (1.4)$$

might be involved via oxidation of the HCN and CN. A number of investigators do not agree with the Fenimore mechanism and suggest super-equilibrium concentrations of O-atoms as a more logical explanation of prompt NO.

Merryman and Levy (15) probed flat methane flames in the presence and absence of nitrogen-containing compounds. Their NO and NO_2 profiles for flames with and without fuel-N additives indicate a sequence of reactions consistent with the mechanism

$$\text{NH and/or CN} + O_2 \rightarrow NO + \text{H and/or CO} \qquad (1.5)$$

$$NO + HO_2 \rightarrow NO_2 + OH \qquad (1.6)$$

$$NO_2 + O \rightarrow NO + O_2 \qquad (1.7)$$

Considering data obtained using a cooled quartz probe, Fenimore (16) in 1975 noticed that in fuel-lean premixed flames at atmospheric pressure and containing about 100 ppm of NO_x the ratio NO_2/NO in the primary reaction zone greatly exceeded the value appropriate to the equilibrium

$$NO + 1/2O_2 \rightarrow NO_2 \qquad (1.8)$$

His work indicates that the equilibrium

$$NO + O \rightleftarrows NO_2 \qquad (1.9)$$

is satisfied in hot enough burned gas from fuel-lean premixed flames.

Since it is unreasonable that equilibrium (9) be maintained by direct attachment and dissociation of O-atoms, he concluded that the reaction

$$OH + NO_2 \rightleftharpoons HO_2 + NO \qquad (1.10)$$

is a plausible way of converting NO_2 to NO and vice versa. This is supported by the fact that the ratio NO_2/NO usually decreases in the burned gas, where the concentrations of O, OH, and HO_2 also decrease.

The results presented by Cernansky and Sawyer (17) in 1975 for turbulent flames also indicate the presence of NO_2. They indicate substantial (around 15 ppm) concentrations of NO_2, which appear to peak slightly on the fuel-rich side. No completely satisfactory explanation for the existence and peaking behavior was found, although they postulate that the formation of nitrogen dioxide occurs through the rapid oxidation of nitric oxide by radicals such as HO_2, which are found in super-equilibrium concentrations.

Sampling probes were used in all these studies, and the authors indicate the strong possibility that the measured NO_2 levels result from reaction within the probe.

Amin (18) discusses the gas-phase reactions of NO to NO_2 in combustion gas sampling probes. Surface effects for oxygen atom recombination in a geometry typical of water-cooled stainless steel aerodynamic sampling probes are considered. He shows that the catalytic activity of the probe walls for atom recombination, the available surface to volume ratio, and the pressure are important parameters controlling the extent of NO_2/NO reactions in the probe environment.

Allen (3) in 1975 probed a premixed methane-air flame above a Botha-Spalding burner and measured the NO and NO_2 profiles. He concludes that the measured NO_2 is a result of a recombination reaction

$$NO + O \rightarrow NO_2 \tag{1.11}$$

which occurs at the probe wall. He also proposes alternative explanations for the NO_2 in the probe samples, for example the initial formation of HO_2 or ozone followed by the oxidation of NO via

$$O \text{ (or H)} + O_2 \rightarrow O_3 \text{ (or } HO_2) \tag{1.12}$$

$$NO + HO_2 \text{ (or } O_3) \rightarrow NO_2 + OH \text{ (or } O_2) \tag{1.13}$$

Allen apparently is the first one, who suggests and proves with his experimental work that NO + NO_2 (NO_x) remains constant as the sample leaves the flame and travels through the probe.

In a later paper, Cernansky (19) in 1976 presents a comprehensive discussion of difficulties in obtaining valid estimates of NO and NO_2 concentrations in combustion systems. He points out that sampling from high-temperature combustion zones (where radical species are abundant) can give in-probe radical relaxation reactions that significantly alter the NO/NO_2 distribution. However, when sampling from relatively cool postflame regions (where radical concentrations are not significant) it appears that the results are not modified due to radical reactions.

Malte and Kramlick (20,21) in 1978 and 1980 presented theoretical and experimental results on the problems of gas sampling for NO and NO_2 in high-temperature flame zones. Their results support the above-

described theory.

Hori (22) in 1980 performed an experimental measurement and a model calculation to study the effects of probing conditions on NO_2/NO_x ratios obtained by a probe sampling from flames. Four quartz probes which were different in sample pressure, cooling rate of sample, and surface-to-volume ratio were used to sample the combustion gases of a premixed CH_4-air flame. He concluded that very low probe pressures (10^{-2} atm) reduce the conversion of NO to NO_2.

The essential problem in gas sampling from high temperature flame zones is that active species such as OH and O are drawn into the sample probe. Due to temperature quench and wall recombinations, these active species are rapidly eliminated from the sample gas stream, but not before they, or less active intermediates such as HO_2, could react with NO or NO_2 and change their concentrations in the gas which eventually is analyzed.

Whatever the mechanism of NO_2 formation in a probe, it is evident that conventional measurements of NO or NO_2 in flames must be performed on samples withdrawn by fine orifice probes. The alternative solution in this problem is spectroscopy. A small number of investigators have used optical methods to perform NO or NO_2 concentration measurements.

Newhall and Starkman (23) in 1967 carried out a theoretical and experimental investigation to determine the mechanism whereby nitric oxide is formed and exhausted from a premixed charge, spark ignition engine. Spectroscopic absorption techniques were used to measure time-resolved in-cylinder concentrations.

Shahed (24) in 1970 measured the rate of formation of nitric oxide in high pressure combustion products. He used ultraviolet absorption spectroscopy (226 nm band) to directly record the time rate of formation of nitric oxide behind a flame front propagating through a premixed charge in a constant volume vessel.

Johnson, Smith, and Mulcahy (25) used a laser-resonance fluorescence technique to make in-situ measurements of NO_2 in a premixed flame. The NO_2 was also measured simultaneously by probe techniques. The true concentration of NO_2 in the flame, as indicated by fluorescence, was considerably less than that indicated by the probe technique. They concluded that the results of probe measurements do not reflect even approximately the true NO_2/NO ratio in the flame.

Zabielski, et al. (26) in 1980 presented a comparative study between the performance of optical and probe-sampling methods for measuring NO in premixed flames. Three combustors were employed. The first was a rectangular, flat flame burner, the second was a swirl stabilized burner, and the third was a modified FT12 (Pratt and Whitney) burner. The results of this work indicate that for gas temperatures up to 2000 K, agreement within about 25 per cent can be expected between results obtained from properly made and interpreted probe and optical measurements of NO.

The motivation for the current work comes mainly from the work of Jaasma and Borman (2), who measured NO and NO_2 concentrations downstream from a steady diffusion flame around a thread wetted with normal heptane. They found that when the air around the flame was doped with

propane or natural gas, the free-stream unburned hydrocarbon concentration had a dramatic effect on the meaured NO concentration. While NO decreased, NO_x (NO_x = NO + NO_2) remained constant. This suggests that NO to NO_2 conversion can occur just outside the flame, where OH or HO_2 may exist due to oxidation of the hydrocarbons doped into the air stream. Because they sampled downstream of the flame, this work does not have probe errors but also does not tell for certain where the NO to NO_2 conversion occurs.

Summary

The preceding indicates that the use of probes destroys the real NO and NO_2 concentrations, while the NO_x (NO + NO_2) concentration remains constant. It seems that most investigators agree that probe reactions such as

$$NO + HO_2 \rightarrow NO_2 + OH$$

lead to a shift between NO and NO_2. It is believed that the observed high concentration of NO_2 is not present in the combustion zone, but arises from reaction in the sampling probe. It is obvious that since the observations inside the flame can be an artifact of reactions occurring in the probes we can not use probes to obtain unquestionable information about NO_2 formation. Spectroscopic measurement techniques could provide a clear answer to the question of how and where NO_2 is formed in combustion systems. Unfortunately, only a few studies have

been published on this type of experimental work. It is significant to notice that in the literature there is no report of spectroscopic, spatially-resolved NO measurements in diffusion flames.

III. EXPERIMENTAL APPARATUS AND INSTRUMENTATION

3.1 Introduction

The purpose of the present work is to make measurements which will enhance our understanding of where NO_2 is formed in combustion systems. In support of this objective, a small diffusion flame has been developed around a liquid-fuel soaked cotton ball to allow conventional measurement of NO and NO_2 concentrations in the gases downstream of the flame. Four types of porous burners which create relatively flat diffusion flames have been tried to evaluate their suitability for spectroscopic NO measurements, while appropriate optical and detection systems have been designed. NO concentrations have been measured using probe and optical techniques. In the following sections, the apparatus for each type of experiment will be discussed separately.

3.2 Spherical Flame Apparatus

Figure 1 shows apparatus which has been set up to allow conventional measurement of the total amount of NO and NO_2 which is formed by a steady diffusion flame around a cotton ball soaked with n-heptane (C_7H_{16}) burning in air or air doped with H_2. The cotton ball burner is mounted between two glass tubes as shown in Fig. 1. The diameter of the cotton ball is about 3 mm, while the diameter and the length of the glass tubes are 5 and 50 cm respectively. The water cooling system shown in Fig. 2 prevents the fuel from boiling. The spherical tank

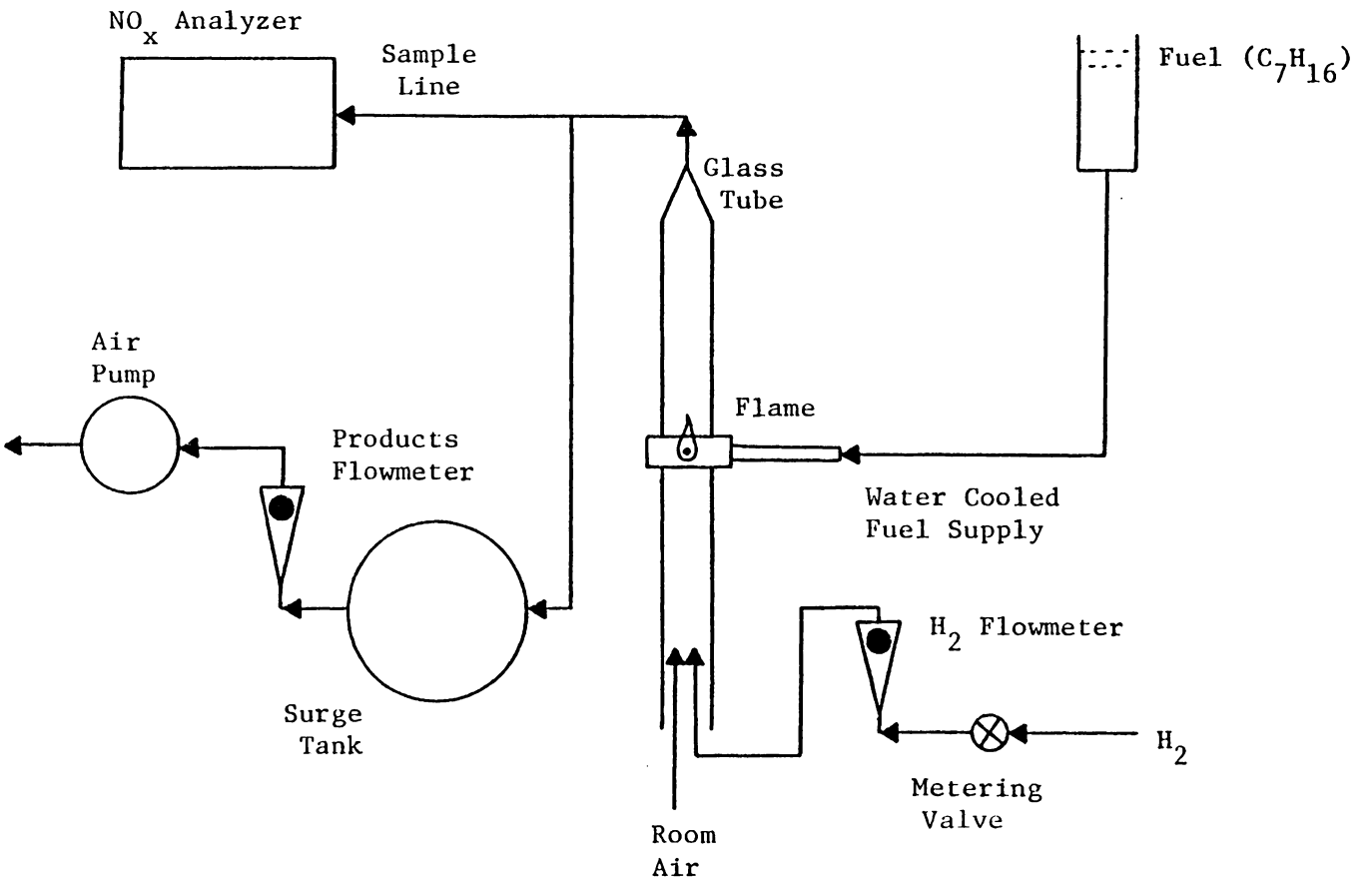

Figure 1. Total NO or NO_2 Measurement System

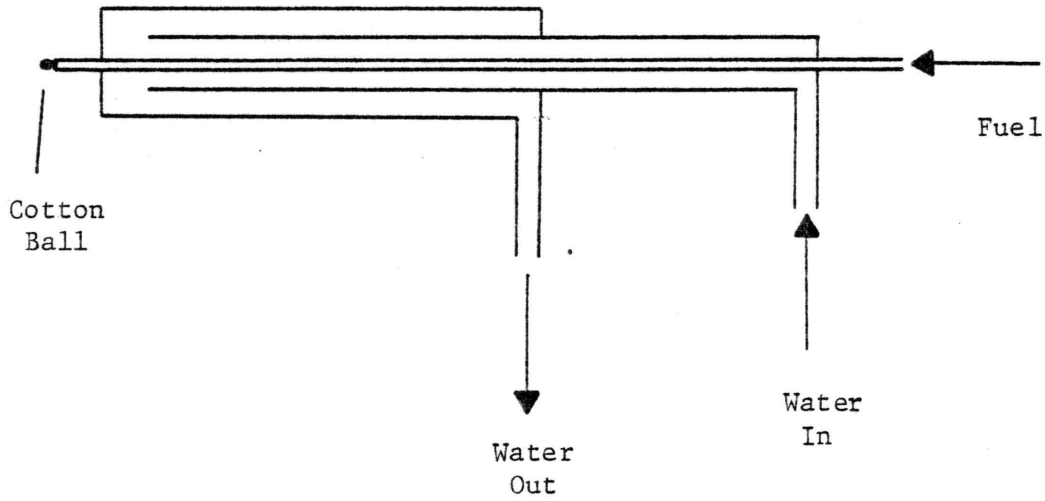

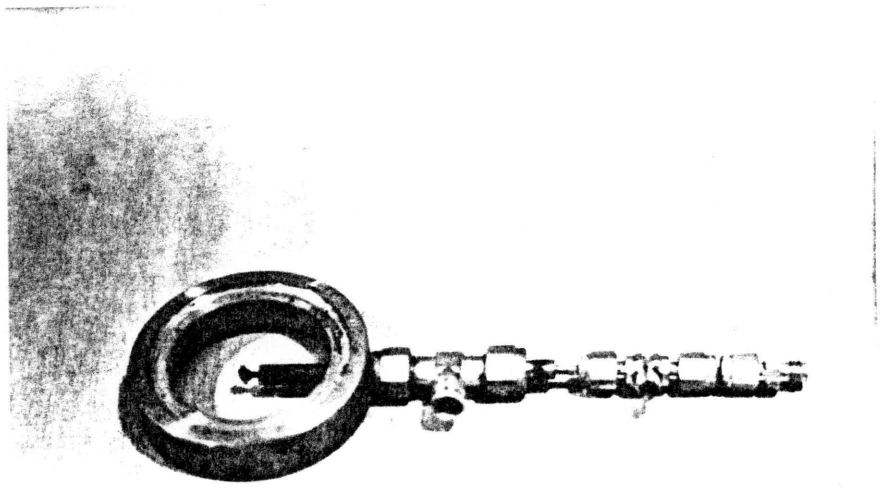

Figure 2. Water Cooling System

before the air pump reduces flow pulsations, producing a steady diffusion flame. The glass tubes protect the flame from surrounding air and drafts. The gas flow to the analyzer is negligible, and thus the rotameters shown can give the hydrogen and product gas flow rates.

3.3 Burners

The flat diffusion flame developed by Wolfhard and Parker (27) has given valuable information about the structure of diffusion flames but is not suitable for the current type of spectroscopic measurement because of the slight premixing of fuel and oxygen which occurs near the base of the flame. Fuel molecules can pass through this small region to the air side of the flame, and this premixing would prevent us from completely controlling the concentration of hydrogen and hydrocarbons in the region outside the flame. One more useful type of flat diffusion flame for the present optical measurements is the counter-flow or opposed-jet diffuson flame of Pandya and Weinberg (27), while porous cylinder burners (28) are also possible.

The first burner used is shown in Fig. 3 and is an uncooled, stainless steel, porous cylinder 15 cm long and 4 cm in diameter. Fuel gas (hydrogen) passes through the porous sides of the cylinder and the flame is maintained in an upward (natural convective) flow of air. There was significantly more heat transfer back to the porous cylinder than had been anticipated, presumably due to infrared radiation from H_2O. The porous surface got hot enough to glow red, and distortion of the porous

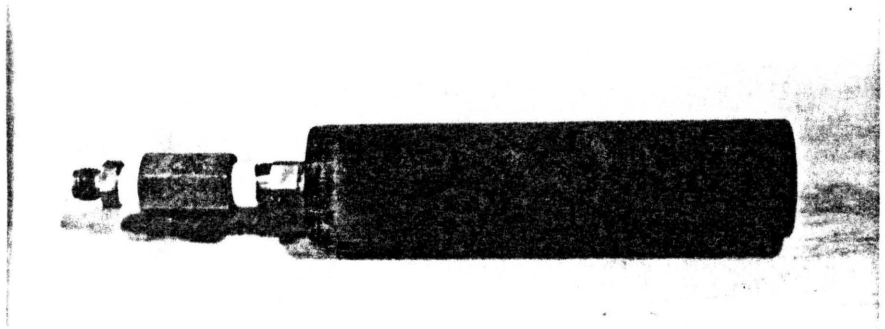

Figure 3. Cylindrical Burner

material was possible. To provide cooling which would prevent the porous metal cylinder from failing, greater H_2 flow rates were tried; this led to a rather unstable flame which appeared unsuitable for the desired type of measurements. A water-cooled version of the porous cylinder was used to cool the cylinder, but the geometry of the flame was disturbed and the porous cylinder burner was abandoned.

The second burner used was the porous disk burner shown in Fig. 4. This burner can be operated with gaseous or liquid fuels and is cooled by a water tube soldered to the fuel chamber. The diameter of the porous surface is 5 cm. Quartz microprobes with a 0.1 mm orifice diameter were used to sample from the flame and measure the NO concentrations, while thermocouples made from 0.025 mm or 0.075 mm diameter Pt - Pt10%Rh wire were used to measure the temperature profile at various locations.

The third combustor used is shown in Fig. 5 and is a rectangular (5 cm x 25 cm) flat flame burner with a water-cooled fuel-supply plenum. The plenum is cut from a brass channel and has two brass rectangular plates soldered on the ends. A porous plate is mounted to the plenum by 12 small screws and the plate is sealed to the plenum with silicone rubber. Mott Metallurgical Corp. porous 316 stainless steel material of 0.5 micron filtration rating and 1.6 mm thickness was used and produced a uniform velocity in the issuing gas, which was H_2 for all the experiments.

The fourth combustor assembly is shown in Fig. 6 and creates an

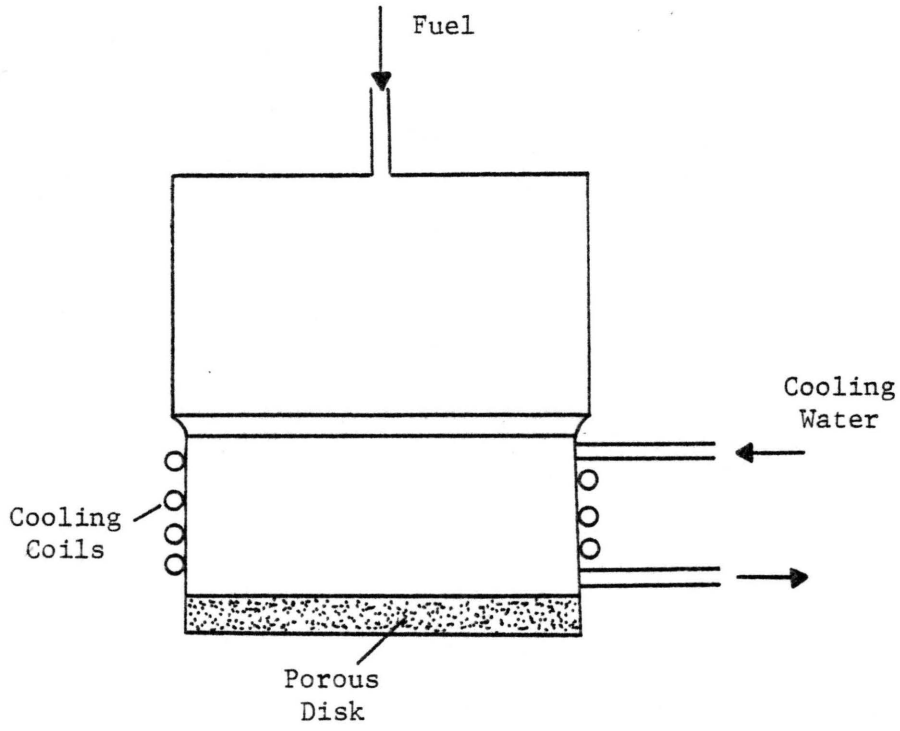

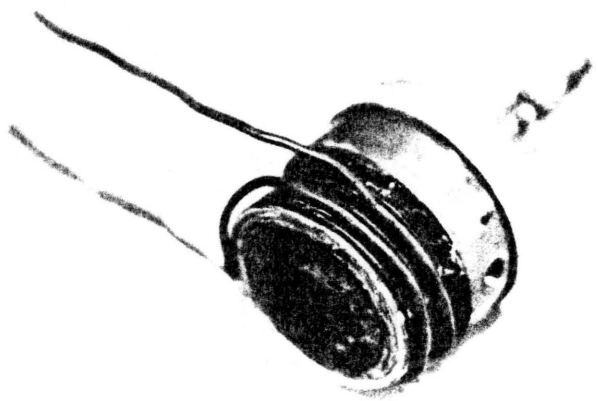

Figure 4. Porous Disk Burner

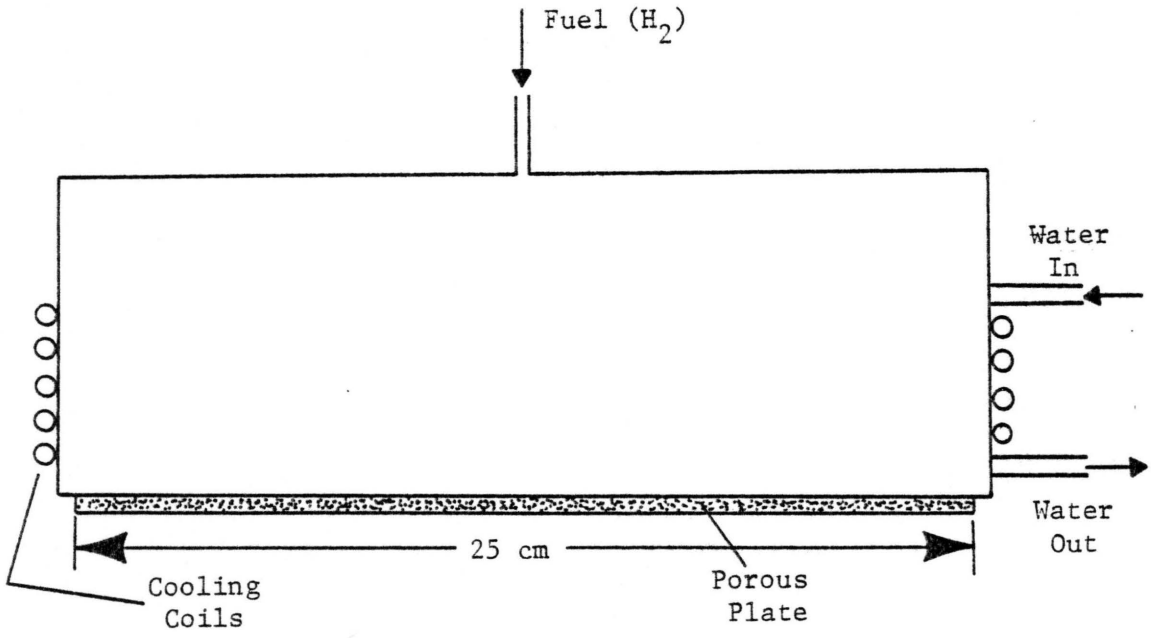

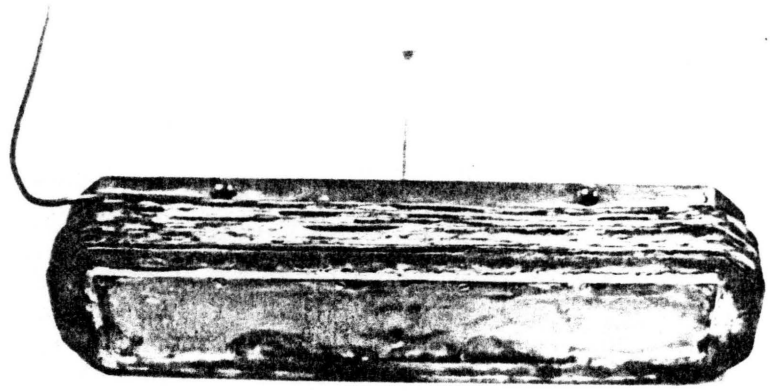

Figure 5. Rectangular Burner

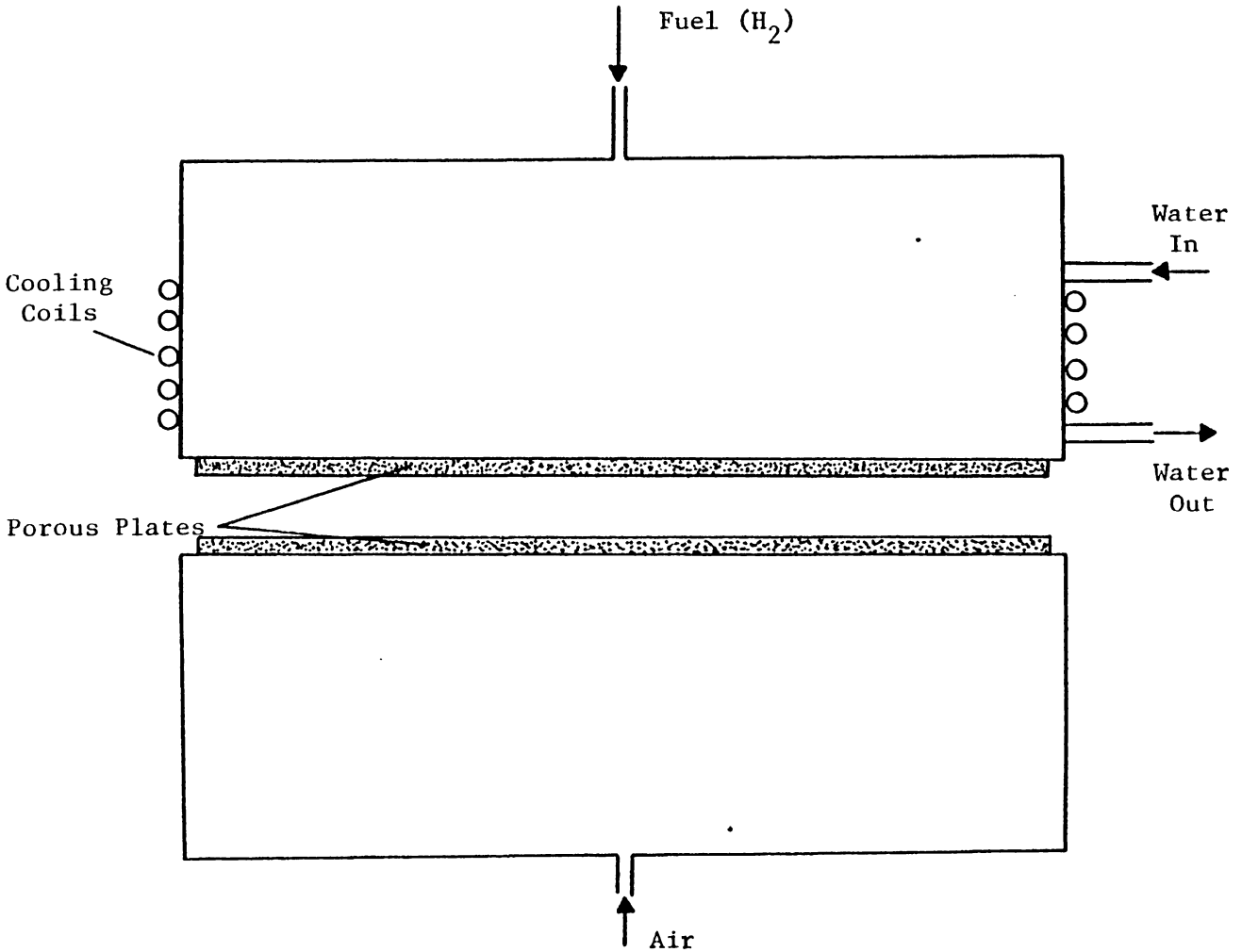

Figure 6. Opposed Jet Burner

opposed-jet flame. This burner consists of the previously described fuel plenum and an air-supplying plenum. The air plenum is exactly as the third combustor, except that the air plenum does not have a cooling system. A gas mixing train was set up and allowed air, NO (450 ppm NO in N_2), and CH_4 (28,300 ppm in air) to be mixed in any desired proportion. The fuel gas was supplied from above through the porous plate, exactly as before, while the air for the flame was supplied from below through the second porous plate. This system, as discussed later, produced a flat, rectangular-shaped flame between the two porous plates and is satisfactory for spectroscopic observations.

The flames of the third and fourth combustors were protected from surrounding air and drafts by an outer Plexiglas jacket as shown in Fig. 7. The figure shows the fourth burner, which was used for the spectroscopic measurements.

3.4 Nitric Oxide and Temperature Probing Equipment

The concentration of nitric oxide was measured by using the sampling system shown in Fig. 8. The system was operated continuously at probe pressures of 0.3 atmosphere and used a 6 mm teflon tube to connect the probe outlet to an electrically heated, stainless steel vacuum pump. The pump was followed by a refrigerated condenser which removed most of the water from the sample. The sampled gas was then directed via an open manifold to the NO_x analyzer. The open manifold prevented pressurization of the input of the instrument. An appropriate traversing

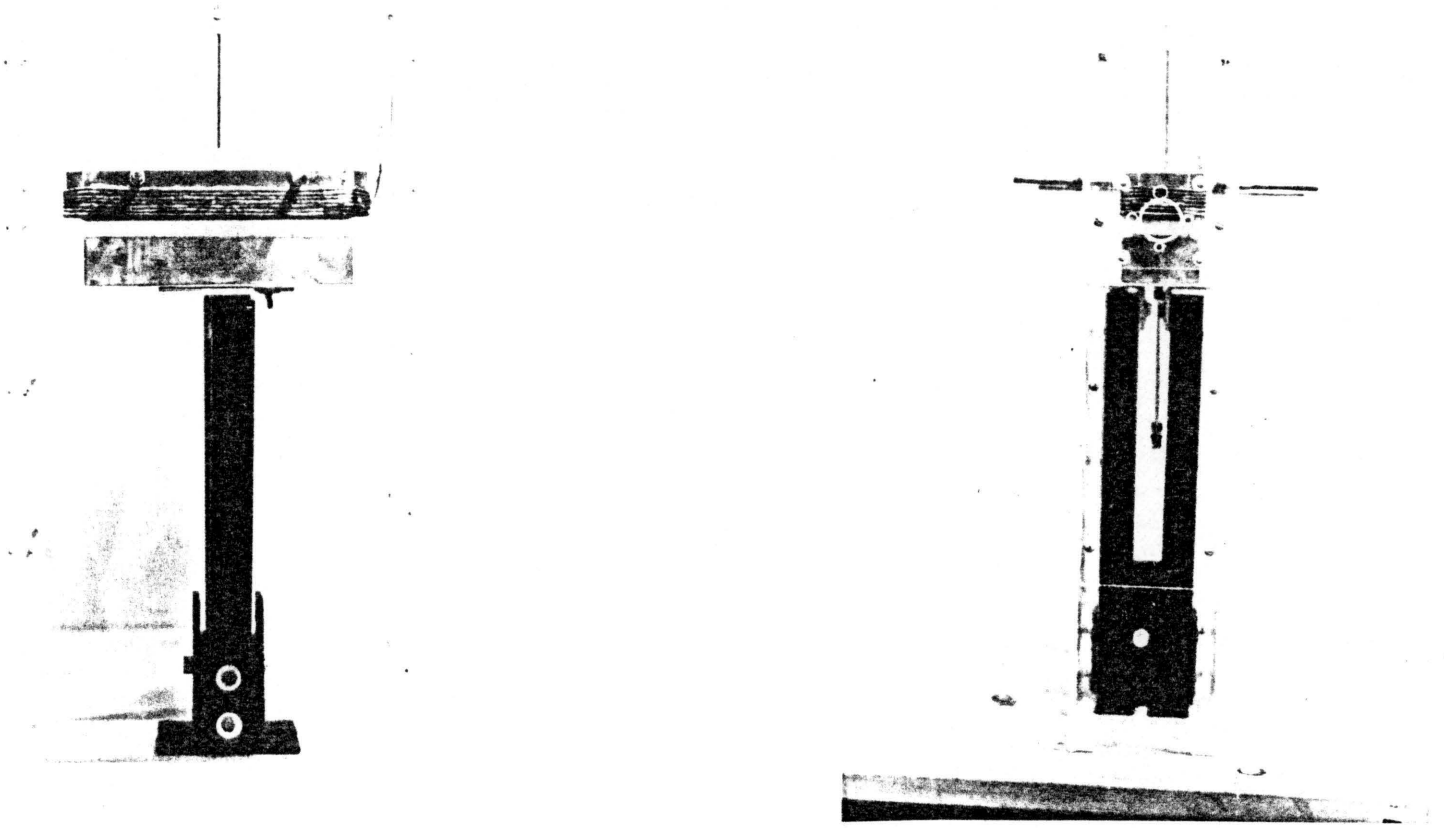

Long Side

Short Side

Figure 7. Flate Flame Assembly

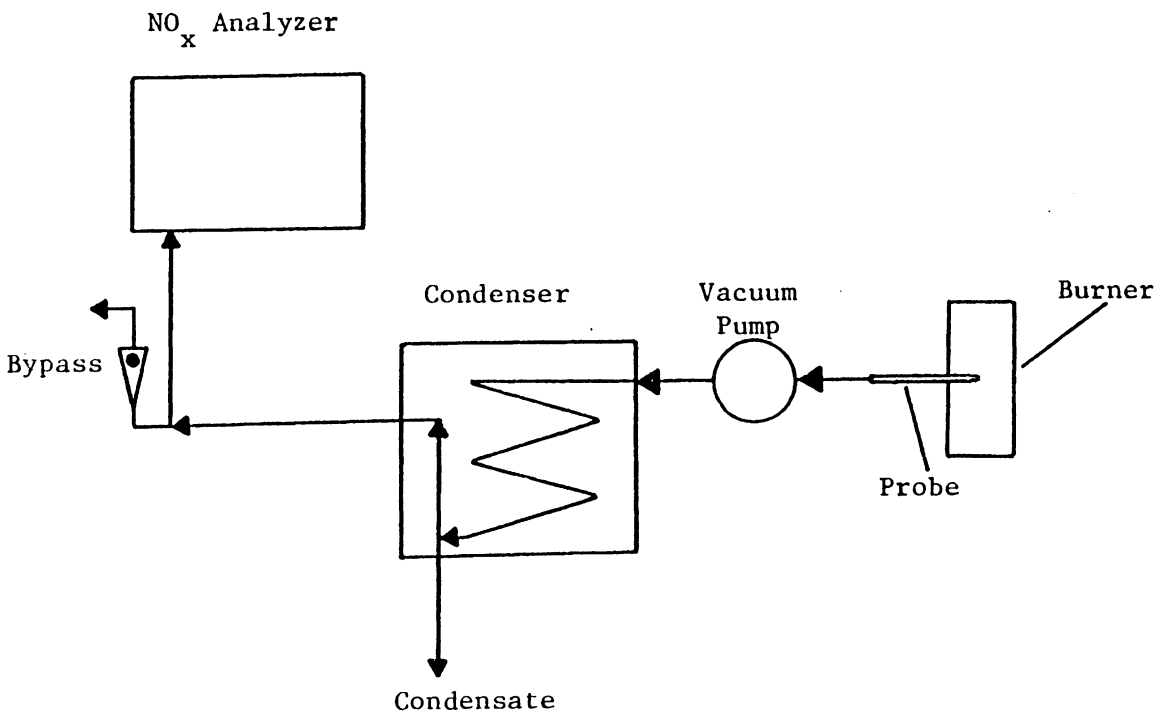

Figure 8. Set-Up for Probe Sampling

mechanism (shown in Fig. 9) allowed combustion gases to be sampled from the flame at any desired position, while the low probe pressure minimized the tendency for NO to be oxidized to NO_2.

A fine Pt vs Pt-10%Rh thermocouple and the same traversing mechanism as before were used to measure the temperature profiles through the flame. Figure 10 shows the thermocouple mounting which was set up to allow vertical and horizontal temperature measurements through the flame.

3.5 Optical System

The set-up for ultraviolet absorption scpectroscopy to measure the in-flame concentration of nitric oxide is shown schematically in Fig. 11, while Fig. 12 gives a photograph of the system. The optical path is parallel to the long axis of the burner. The optical system consists of an ultraviolet light source, condensing lenses, transmission windows, horizontal slit, and monochromator.

A Hanau D 120 F deuterium lamp was used as an ultraviolet light source. This lamp provides a continuous, line-free radiation spectrum from 195 nm to 350 nm and requires a starting voltage of 320 Volts DC and a running voltage of 100 Volts at 0.3 or 0.6 Amperes, depending on whether the lamp is run at 30 or 60 Watts. A Gates DCR 30/60 G deuterium lamp power supply meets these requirements and was used at the 30 Watt setting. The deuterium lamp is mounted on a frame parallel to the long axis of the burner, as shown in Fig. 13, and can be fixed at any desired position.

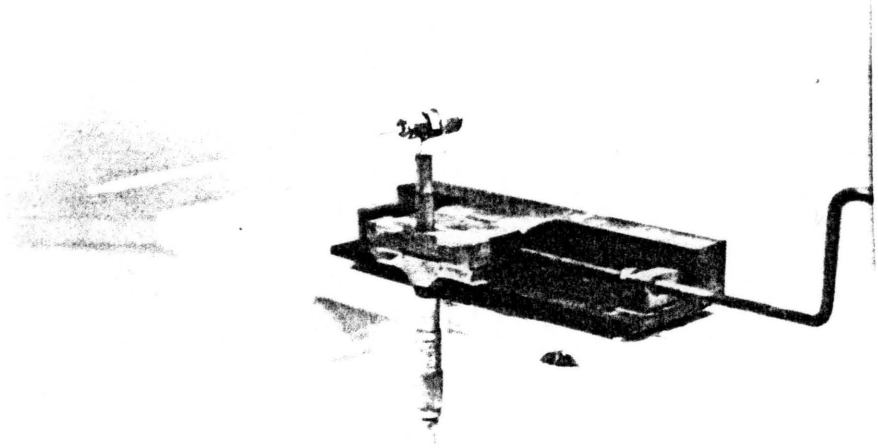

Figure 9. Probe with Traversing Mechanism

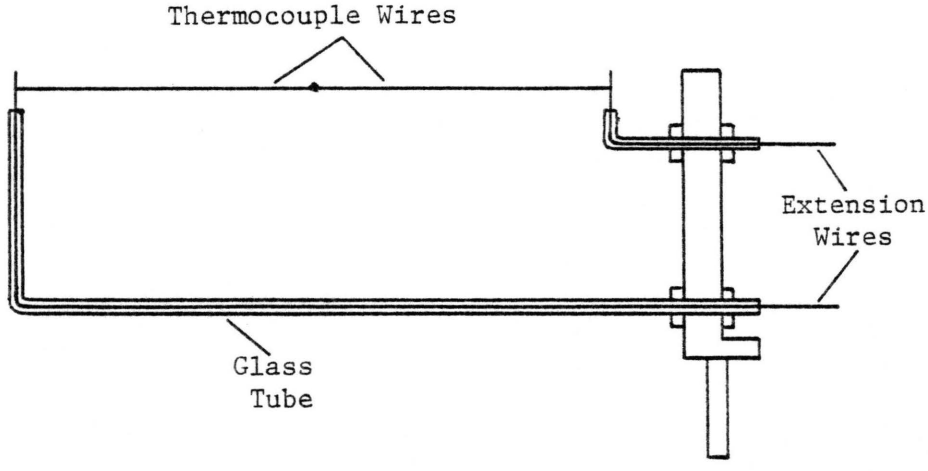

Figure 10. Thermocouple Mounting

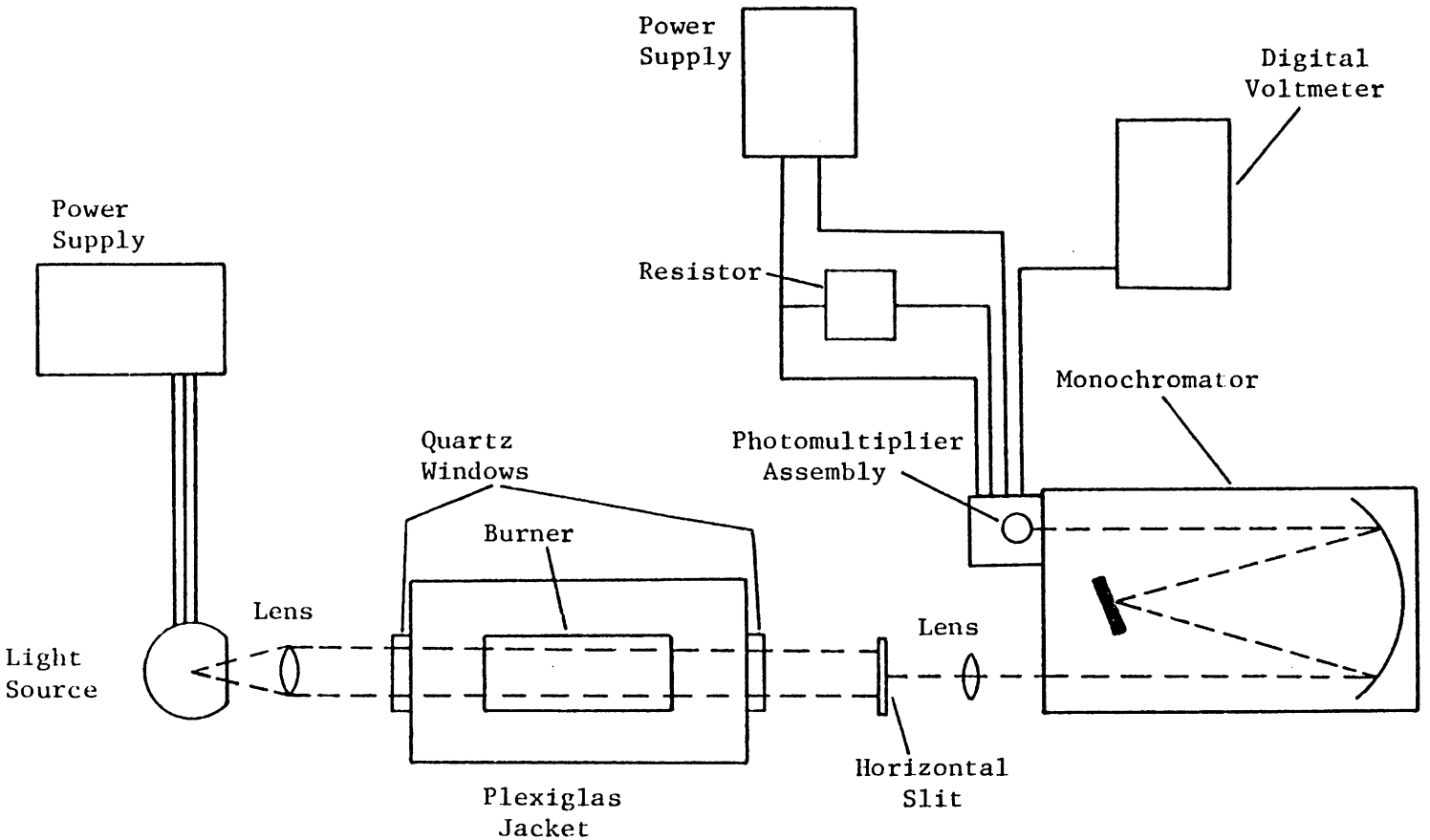

Figure 11. Top View of Optical System

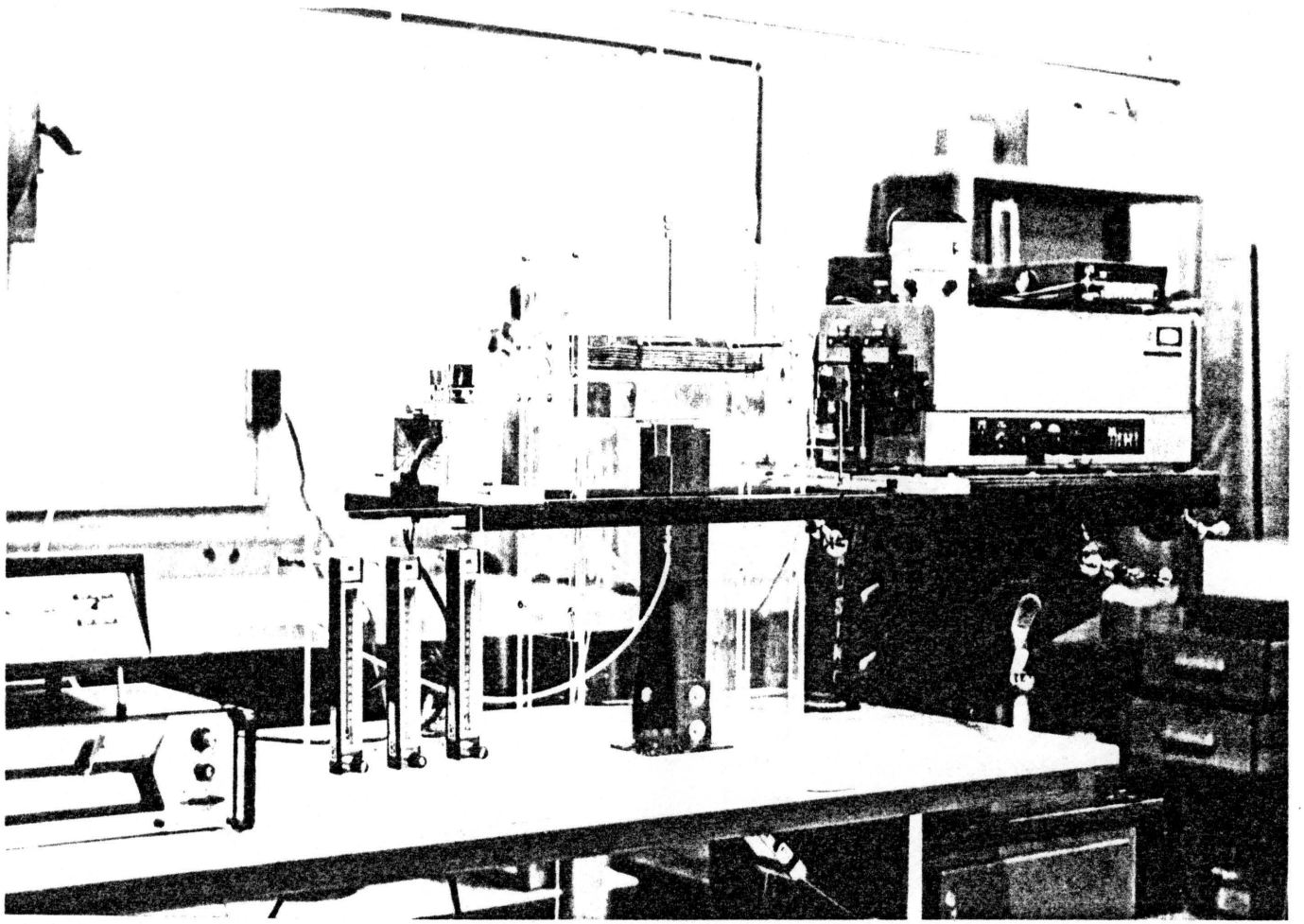

Figure 12. Photograph of the System

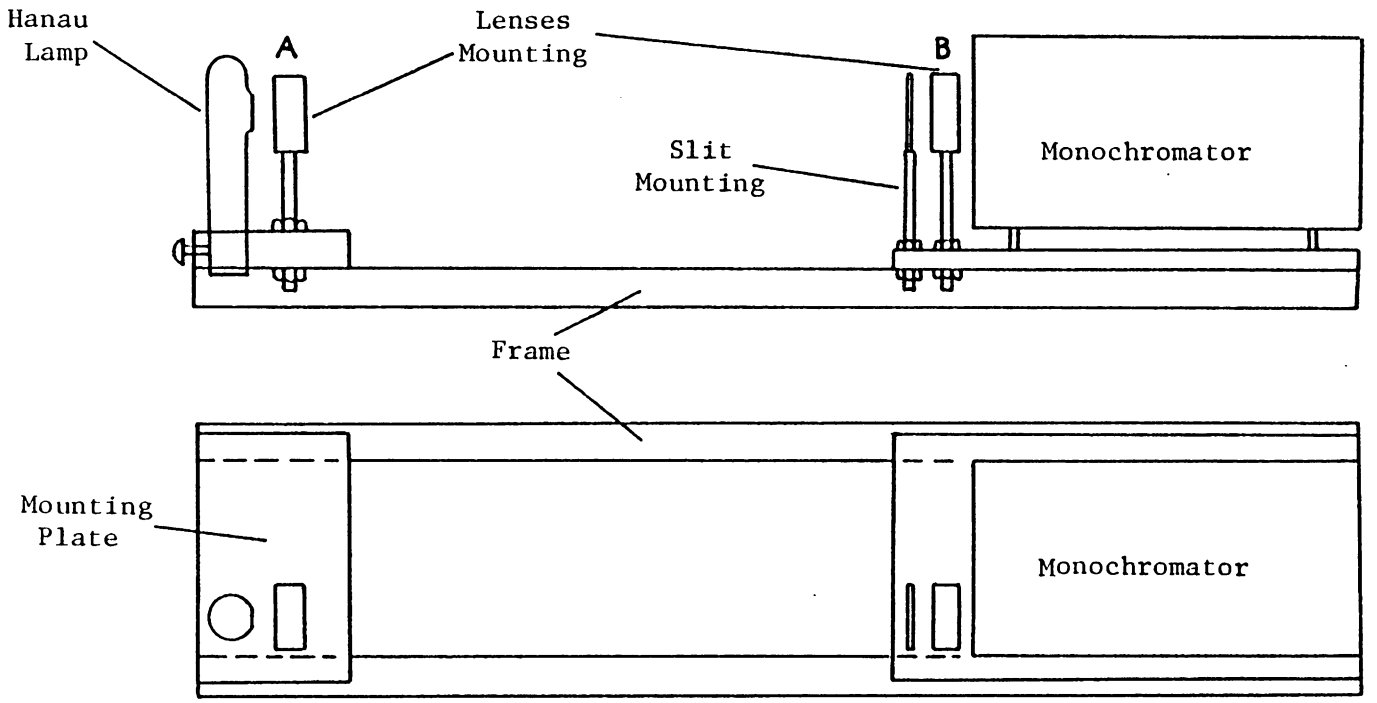

Figure 13. Mounting of Optical System

The condensing system consists of two Spectrosil B biconvex lenses of 25 mm focal length and 22.4 mm diameter. The mounting of the lenses is shown in Fig. 13. The lens A is placed after the ultraviolet light source, while the lens B is located in front of the monochromator entrance slit. The height of the lenses can be adjusted through the adjusting nuts as shown. The distance of the lenses from the light source and the monochromator can be adjusted by moving them along the slot in their mounting plates. These adjustments permit the proper alignment and focusing on the optical path.

Two diametrically opposed, ultraviolet-grade quartz windows are mounted on the Plexiglas enclosure. The layout of the optical system can be seen from Fig. 11. Light from the deuterium light source is collimated, passes through the flame, and is then focused onto the inlet slit of a Jarrel Ash 82-020 half metre scanning spectrometer which has adjustable entrance and exit slits and a diffraction grating having 1180 grooves/mm. The specified dispersion is 16 Angstroms per mm.

The diameter of the optical beam through the flame is about 2 cm, since the diameter of the lenses is 2.24 cm. This type of beam is unsuitable for space-resolved measurements in a diffusion flame at ambient pressure. A narrow horizontal slit (0.8 mm x 5 mm) blocks most of the beam and allows the appropriate measurements. The optical system (except for the windows) is mounted on a milling machine table which is used to move the whole system up and down in space and allows measurements at various elevations through the flame without re-aligning the optical system.

3.6 Detection and Recording Systems

Monochromatic light (more precisely, of a finite bandpass) emerges from the monochromator exit slit and strikes the detector, an RCA Bialkali 4837 photomultiplier tube. An RCA PF 1042 power supply is used for the tube. The cathode absolute responsivity (mA/Watt) of the tube is maximum from 180 to 300 nm. The PF 1042 provides a regulated output voltage (-500 to -1000 Volts) which is controlled by a variable resistance (0 to 500 kΩ). The photomultiplier tube output voltage (across a 2 kΩ resistor) is displayed by a Heath SR-204 chart recorder or a digital voltmeter.

IV. EXPERIMENTAL PROCEDURES

4.1 Spherical Flame

The experiment is shown schematically in Fig. 1 and involved a steady diffusion flame around a cotton ball wetted by a constant flow of C_7H_{16}. The flame was in air at ca. 0.9 atmosphere and was spherically symmetric at the base, but above the equator the flame gradually degenerated into the familiar free convection plume. The pump induced an air flow which supported the flame. After mixing with the air around the flame, the combustion products' NO and NO_2 concentrations were measured. At the same steady fuel flow rate, the air entering the bottom of the glass tube was doped with hydrogen and the concentrations of NO and NO_2 were measured again. The amount of H_2 added to the air stream determined the concentration of H_2 (0 to 8000 ppm) in the approach stream. The overall product gas flow was maintained at 10 liters/minute.

4.2 Optical Calibration

The spectrum of a mercury vapor lamp was used to check out the optical system. The corespondence of the peaks shown in Fig. 14 with the known wavelengths of the mercury spectrum is evidence that the spectrometer grating had been satisfactorily installed and adjusted. As a further check of the system, the spectral output of the deuterium lamp was measured. The agreement between the measured output and the

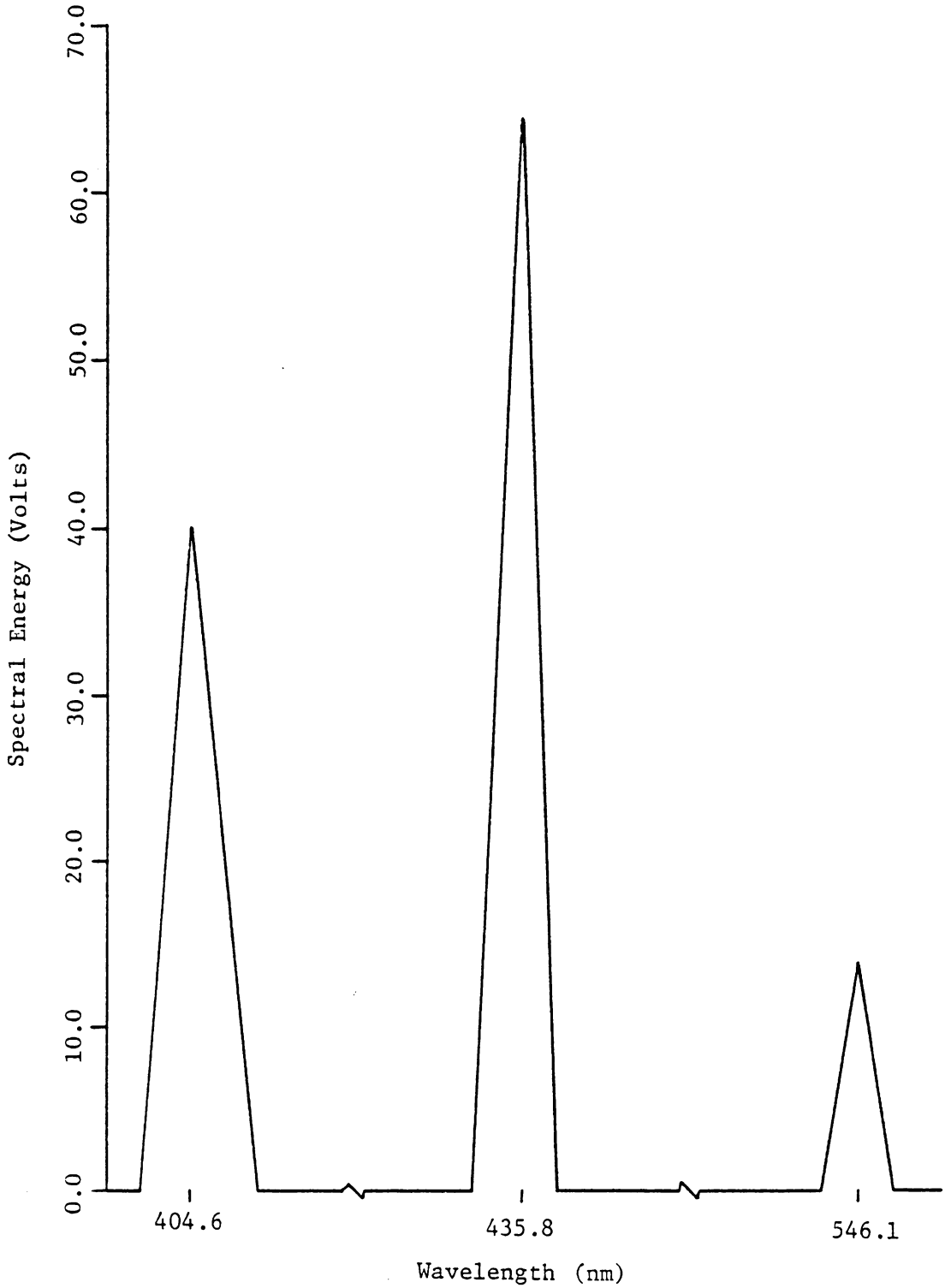

Figure 14. Spectral Energy of Mercury Lamp Monochromator slit height and width 20 and 2 mm relatively

manufacturer-supplied curve is quite good, as is shown in Fig. 15.

The concentration of nitric oxide in the optical path of the flame is determined from the recorded spectral absorption due to the (0.0) and (1.0) gamma band of nitric oxide near 226 and 215 nm. Figure 16 shows the apparatus which was set up to allow calibration measurements. The collimated ultraviolet radiation beam from the deuterium lump passed through the quartz windows (parallel with the long axis of the glass tube) and was focused on the entrance slit of the spectrometer. Mixtures of nitric oxide (500 ppm NO in N_2) and nitrogen were flowed through the glass tube and the NO concentrations were measured using a Bendix model 8102 NO_x analyzer. The voltmeter readings for the various mixtures were recorded.

Calibration data were fit to a Lambert-Beer (29) law of the form

$$A_\lambda = 1 - \exp(-K_\lambda \cdot C \cdot L) \qquad (4.1)$$

where

A_λ = spectral absorption at wavelength λ

K_λ = spectral absorption coefficient at wavelength λ $(\text{ppm cm})^{-1}$

C = concentration of nitric oxide (ppm)

L = length of optical path

The value of the per cent spectral absorption A_λ as determined by the calibration procedure depends upon wavelength, nitric oxide concentration, temperature, and the monochromator band pass. During the calibration procedure monochromator wavelength was held constant at two

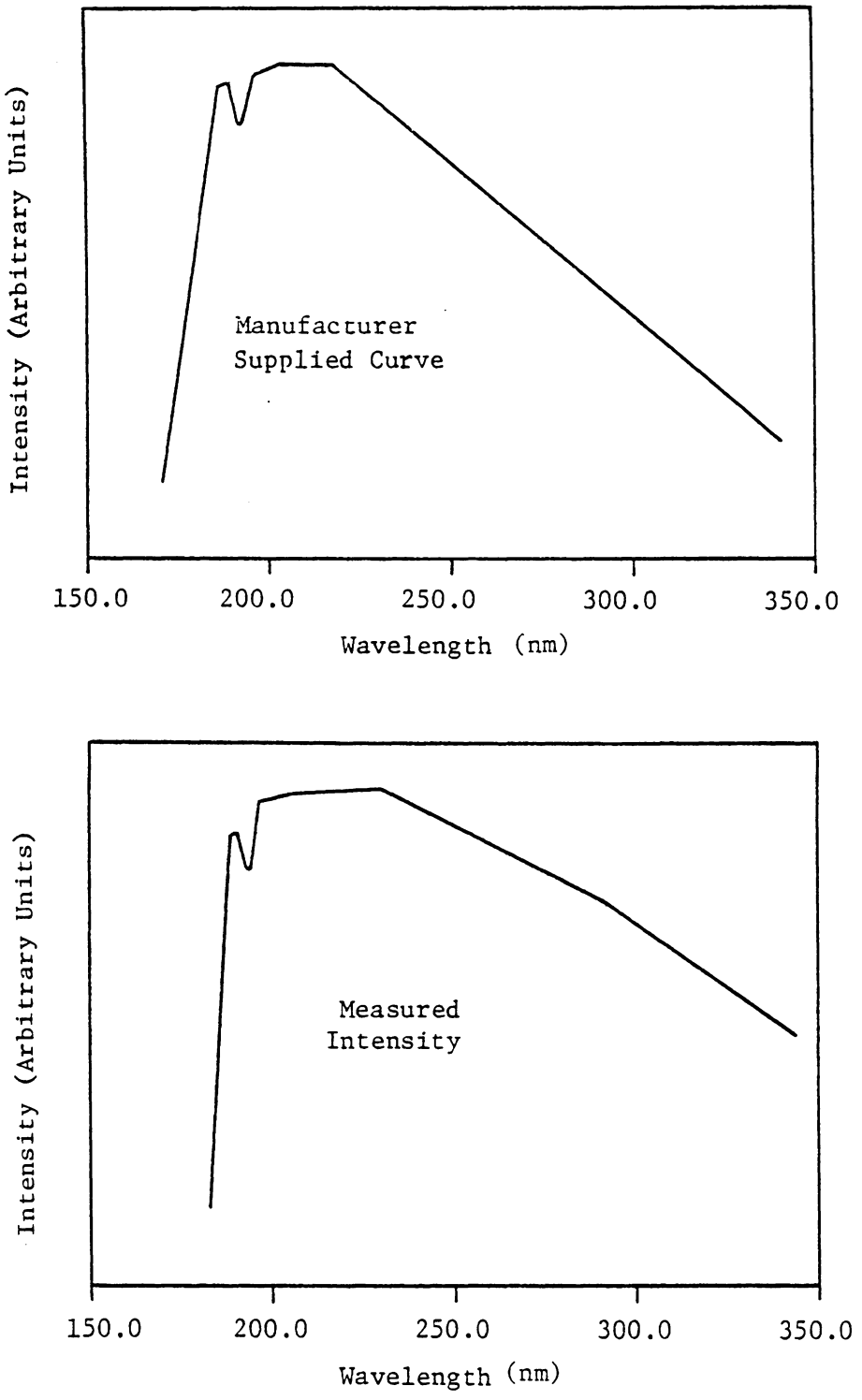

Figure 15. Spectral Energy Distribution of Deuterium Lamp Monochromator slit height and width 20 and 2 mm respectively

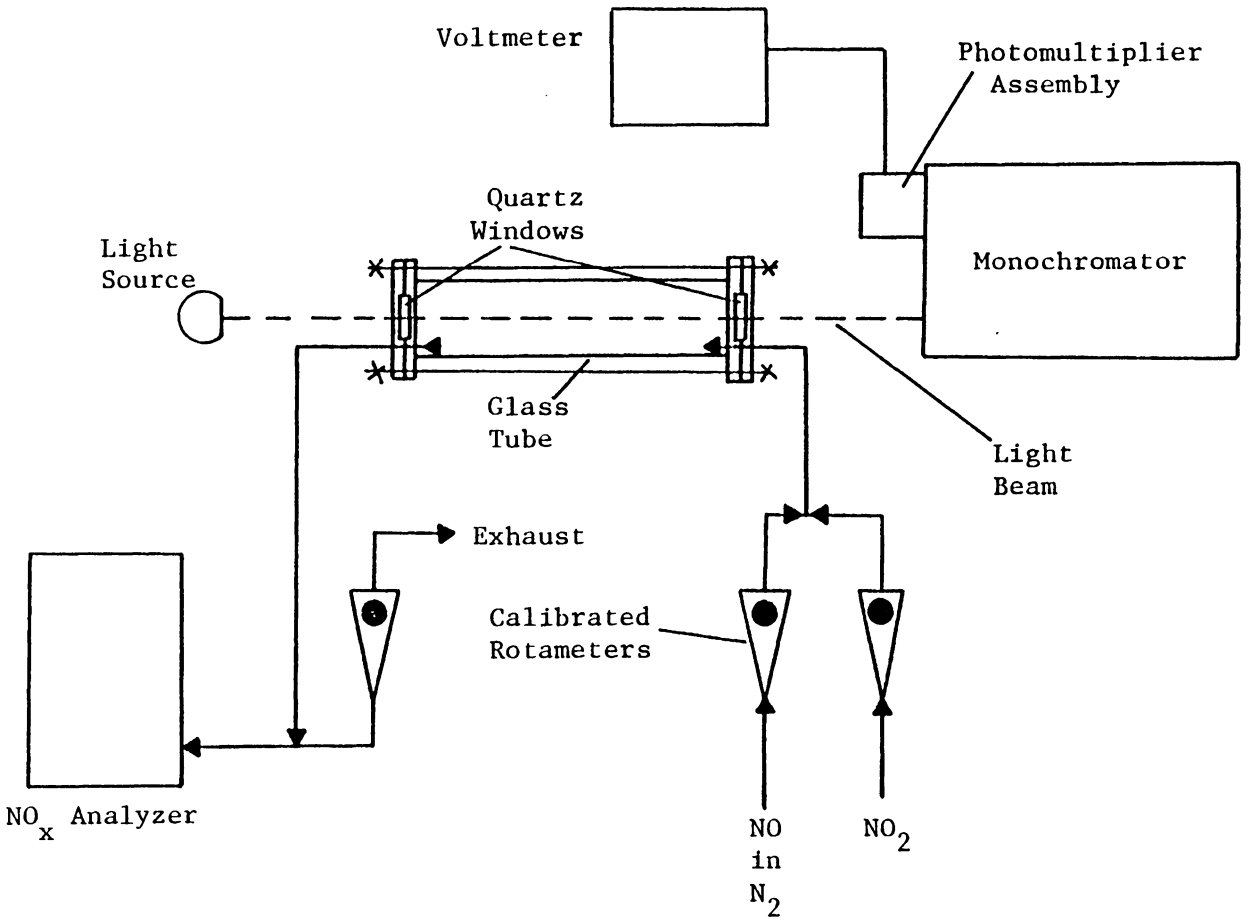

Figure 16. Calibration Apparatus

positions (214.8 and 226.2 nm) and the per cent spectral absorption was found as a function of nitric oxide concentration and bandpass (slit width) of the monochromator. The slit height was constant at 2 cm.

The values obtained from the calibration tests were used in conjunction with the Lambert-Beer law to obtain the spectral absorption coefficient $K_\lambda(C)$ as a funtion of NO concentration and monochromator bandpass as independent variables. It is realized that calibration results obtained under flame temperatures would be more accurate. However, due to time constraints and experimental difficulties the calibration was performed at room temperature. In contrast, experimental data were obtained at temperatures up to 1700 K. A temperature correction based on the equilibrium depopulation of the ground vibrational state at flame temperatures was applied to the calibration. The appropriate calculations are shown in Appendix 9.1.

4.3 Variation of the Refractive Index with Temperature at Constant Pressure

The refractive index is a strong function of temperature according to the relation

$$(n - 1) \propto \frac{1}{T} \quad \text{or} \quad \delta_T = \frac{T_o}{T} \delta_o \tag{4.2}$$

where

$$\delta = n - 1$$

and the suffix 0 denotes the reference state (N.T.P.) at which δ is of the order 0.0003. The refractive index gradient is important because it will cause the light from the deuterium lamp to follow a curved path through the flame, causing confusion about where in the flame the optical path is. It was desired to estimate the magnitude of this effect. Figure 17 shows the end view and side view of a porous cylinder which was supplied with H_2 from the inside and was used to produce a natural convection diffusion flame. The flame was nominally of the shape shown in the sketch, roughly cylindriical in the lower half. A 0.075 mm diameter Pt Vs.Pt-10%Rh thermocouple and a suitable traversing mechanism were used to measure the temperature profile through the flame. The measured temperature profile was used to estimate the value of $\frac{dn}{dr}$. The refractive index gradient, in conjunction with the relation

$$R = -\frac{n}{\frac{dn}{dr}} \tag{4.3}$$

was used to give the radius of curvature.

4.4 Flate Flame Burner

Experimental procedures used in comparing the performance of optical and probe sampling methods for measuring NO concentrations for the cases of undoped air and air doped with CH_4 or H_2 are described herein.

4.4.1 Probe Testing

The NO concentration and temperature profiles were taken for the

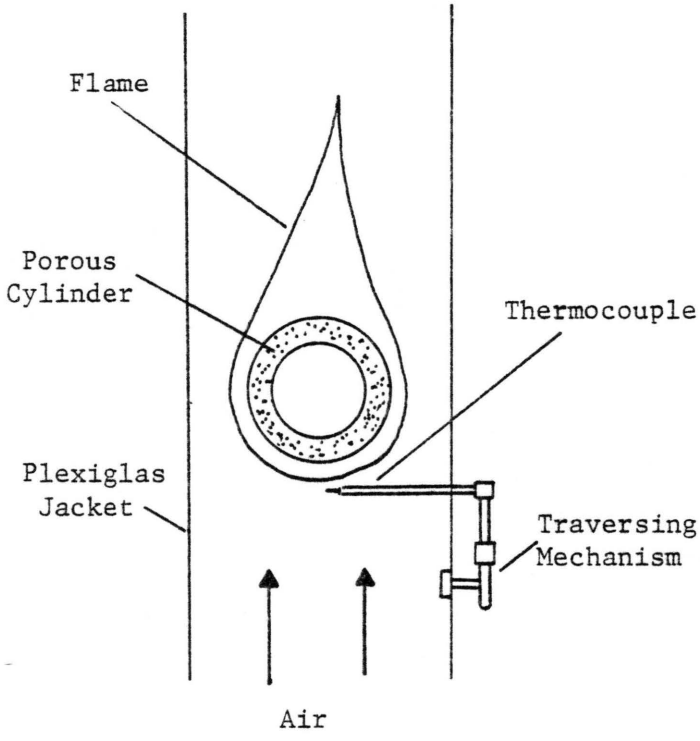

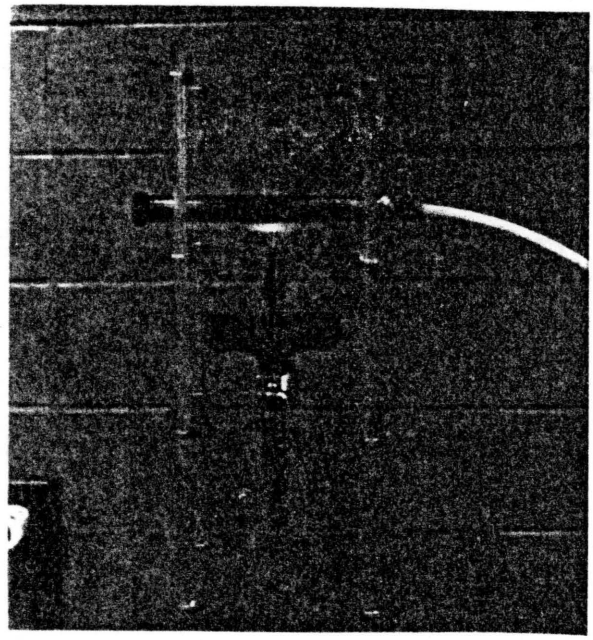

Figure 17. Porous Cylinder with Thermocouple and Traversing Mechanism

three flat burners with similar experimental procedures. The mixture of fuel and air was ignited under the burner and a flat diffusion flame developed. The water valve remained open to provide cooling of the burner. The conventional probe system was operated continuously at probe pressures of 0.3 atmosphere and was used to obtain vertical and horizontal profiles of nitric oxide in the flame.

For the opposed jet burner, the ratio of fuel to air plus NO was varied. The strength of the mixture was changed until a flat flame was created with flow rates of 20 l/min for air, 5.7 l/min for NO in N_2, and 1.2 l/min for fuel. The distance between the air plenum and the fuel plenum was adjusted to 15 mm, a value which was used for all subsequent tests with the opposed jet burner. Flame gases were again sampled through the quartz probe at various heights between the two porous plates. At the same fuel flow rate the flame was doped with measured amounts of CH_4 and the NO concentration profile was measured again. The zero and span of the NO_x analyzer were checked to ensure that the analyzer drift was within acceptable limits.

Flame temperatures were measured by fine (0.075 mm diameter wire) thermocouples and were not corrected for radiation effects.

4.4.2 Optical Testing

Start-up procedures for optical measurements were similar to those for probe testing.

All the types of burners were tried to evaluate their suitability for in-situ measurements, which were begun only after a suitable flame

was produced. Figure 18 shows the opposed jet burner which was set up to allow optical measurements of NO concentration. Ultraviolet radiation was emitted from the deuterium lamp and traveled as a light beam parallel to the flame surface. The part of the beam passing through a narrow, rectangular (0.8 mm high x 5 mm wide) slit was focused on the entrance slit of the monochromator. The monochromator grating was set at the nitric oxide absorption wavelength (214.8 nm). The nitric oxide which was formed as a result of combustion absorbs light of this wavelength, and the NO concentration was measured by measuring the absorption of ultraviolet light passing through the flame. The width of the monochromator slits was maintained at 0.1 mm, gives which a bandpass of 0.16 nm. The optical beam was moved up and down and detected the NO concentrations above, inside, or under the visible reaction zone. At the same fuel flow rate, the air supply was doped with measured amounts of CH_4 and the concentrations of NO were measured again.

4.5 Study of Interfering Spectra

The Schumann-Runge bands of oxygen absorb ultraviolet radiation in the vicinity of 200 nm. With heated oxygen the absorption extends to much longer wavelengths, as far as 260 nm in hot flames with excess oxygen. It has been observed by other investigators (30) that the Schumann-Runge bands appear as a continuum at the temperature and concentration conditions occuring in the present flame. For this reason a careful study of background absoprtion in the vicinity of the (1,0) and

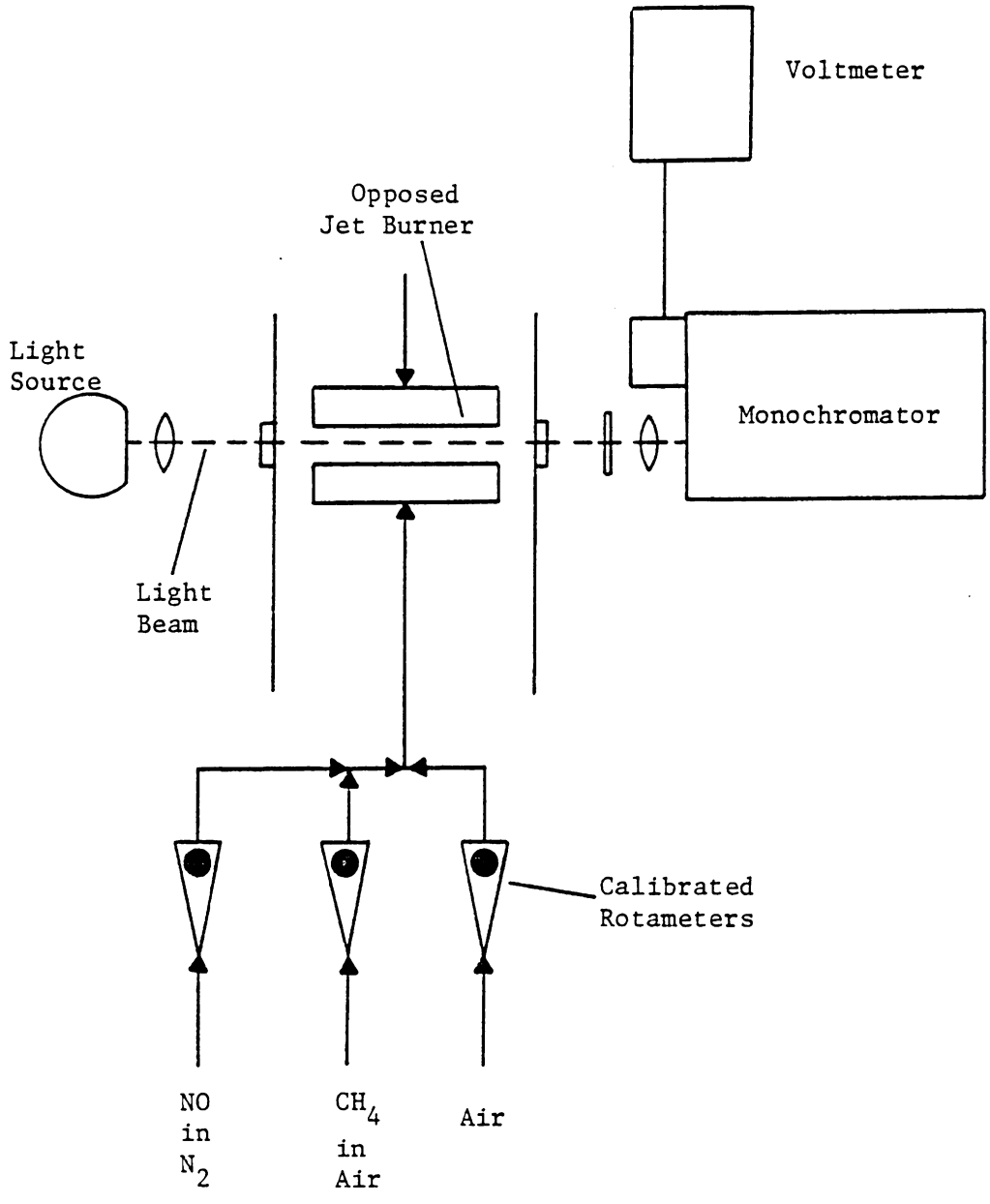

Figure 18. Set-Up for Spectroscopic Measurements

(0,0) gamma bands of nitric oxide was performed. All experimental runs for optical measurement of nitric oxide include simultaneous measurement of background absorption, and the relative levels of background and nitric oxide absorption are measured. $A_{background}$ and A_{total} at the nitric oxide gamma band frequency are determined, where $A_{background}$ represents the fractional absorption due to hot oxygen alone and A_{total} represents the total fractional absorption due to nitric oxide and hot oxygen. Background correction is effected by a logarithmic subtraction based on the following equations (24):

$$A_{background} = 1-\exp(-k_{\lambda} \cdot C_{O_2} \cdot L) \tag{4.4}$$

$$A_{total} = 1-\exp(-k_{\lambda} \cdot C_{O_2} \cdot L - K_{\lambda} \cdot C_{NO} \cdot L) \tag{4.5}$$

Rearrangement and subtraction of equations (4.6) from (4.7) gives

$$C_{NO} = \frac{1}{K_{\lambda}(C) \cdot L} \ln \frac{1 - A_{background}}{1 - A_{total}} \tag{4.6}$$

Equation (4.8) is then solved for C_{NO} employing the spectral absorption coefficient K generated during system calibration.

V. RESULTS AND DISCUSSION

5.1 Introduction

Before giving the results, it is well to reiterate several points. With the use of the spectroscopic technique, it was desirable to minimize the existence of temperature and concentration gradients along the optical path. A flat flame burner is therefore required. The NO profile was measured by making use of ultraviolet absorption due to the (1,0) and (0,0) gamma bands of nitric oxide in the vicinity of 215 nm and 226 nm. Initial estimates and subsequent measurements indicated that to ensure a significant optical absorption, the flame must be seeded with NO. The traversing mechanism allowed measurement of NO on the air side and on the fuel side of the flame. These measurements indicate whether NO is destroyed in the region around the flame. Measured temperatures and NO_x concentrations using conventional methods for different types of flames and burners are used to help document the conditions of the phenomenon.

5.2 Estimated Curvature of Light Beam

As discussed in section 4.4, if the extremities of an element of wave front continue to travel in media of different refractive index the element will progressively change direction. The experimentally measured temperature profile (for the porous cylinder flame) which is given in Fig. 19 was used in conjunction with equation 4.4 to estimate the rate of change of refractive index with the vertical distance from the

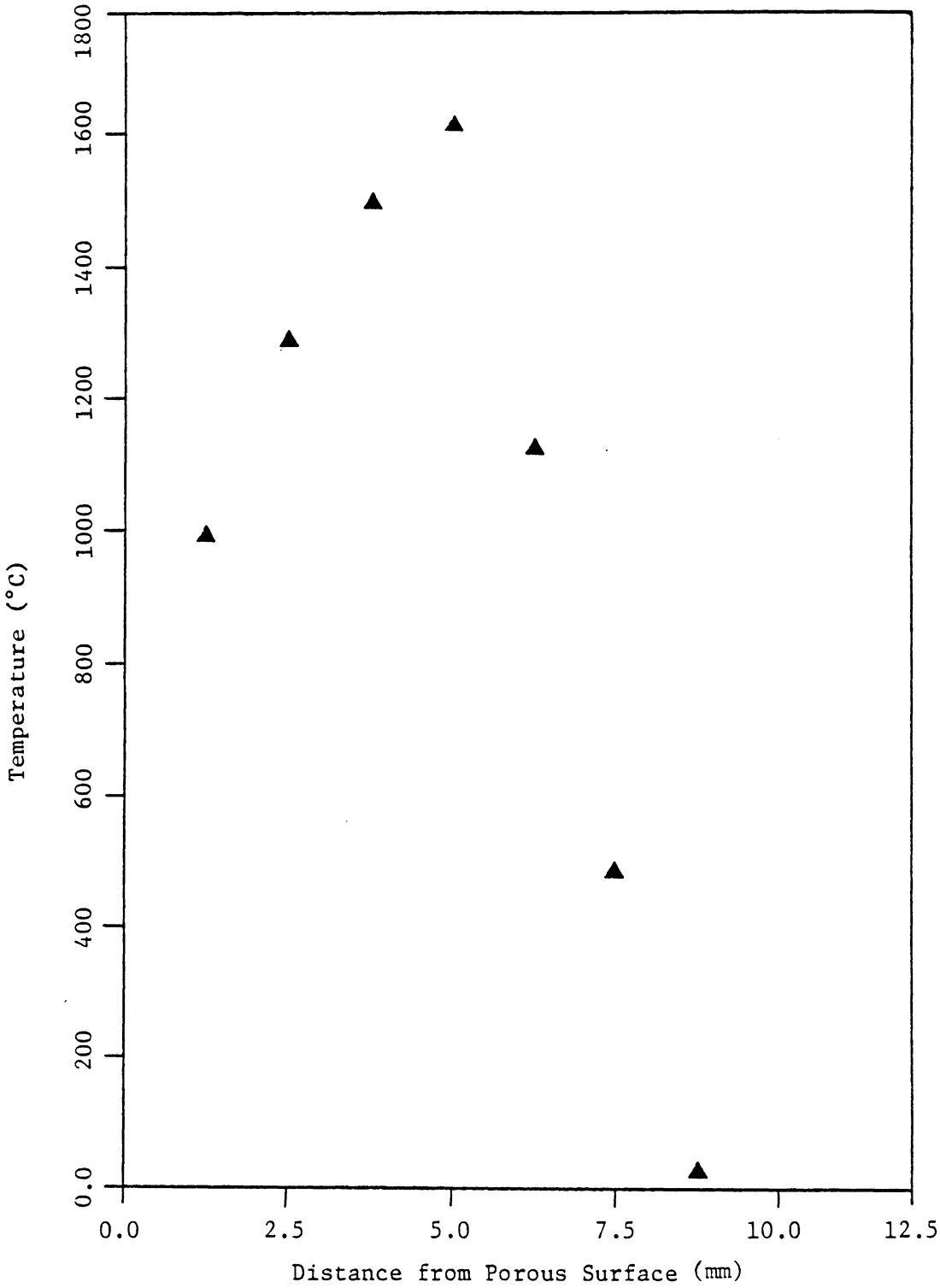

Figure 19. Temperature Profile for H_2-Air Diffusion Flame, Around 1 cm Diameter Porous Cylinder. No radiation corrections, 0.075 mm thermocouple wire

burner. The results are given in Fig. 20. The maximum refractive index gradient (0.052 m^{-1}), the relative refractive index in the air side of the flame (1.00012), and expression 4.5 were combined to obtain the smallest (worst case) radius of light beam curvature, which is 19 m. Thus the beam deflection will reduce spatial resolution but will not necessiate use of a curved porous surface to create a curved flame, which might allow the light beam to follow a line of more constant concentration in the flame. The measured gradients of temperature for the flat burners are even smaller than for this burner, and consequently the radius of curvature of the light beam through the flame becomes larger and the assumption is even more reasonable.

5.3 Temperature Profiles of Flat Burners

The first flat burner creates a stable diffusion flame with an (apparently) thick visible reaction zone. The thickness of the visible zone appears (due to curvature) to be about 2 or 3 mm near the center of the porous disc plate and appears to narrow to about 1 mm near the disc's rim. Figure 21 gives the radial measurements of temperature at two different elevations on the z axis of the burner, just under the visible reaction zone. It is important to note again that with spectroscopic absorption techniques, the concentration of nitric oxide can only be determined for an optical path which is isothermal. In contrast, the radial (horizontal) temperature profiles show significant temperature gradients and it is concluded that this type of flame is not suitable

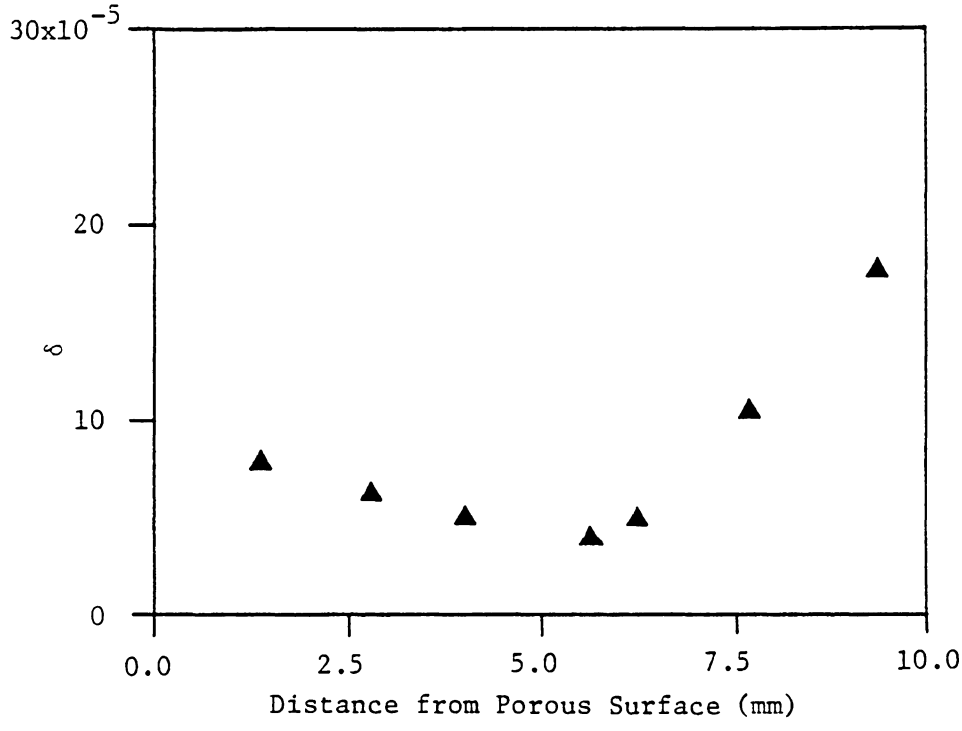

Figure 20. Refractive Index Profile for Natural Convection H_2-Air Diffusion Flame around 1 cm Diameter Porous Cylinder.

■ 5 mm From the Porous Disk

● 6 mm From the Porous Disk

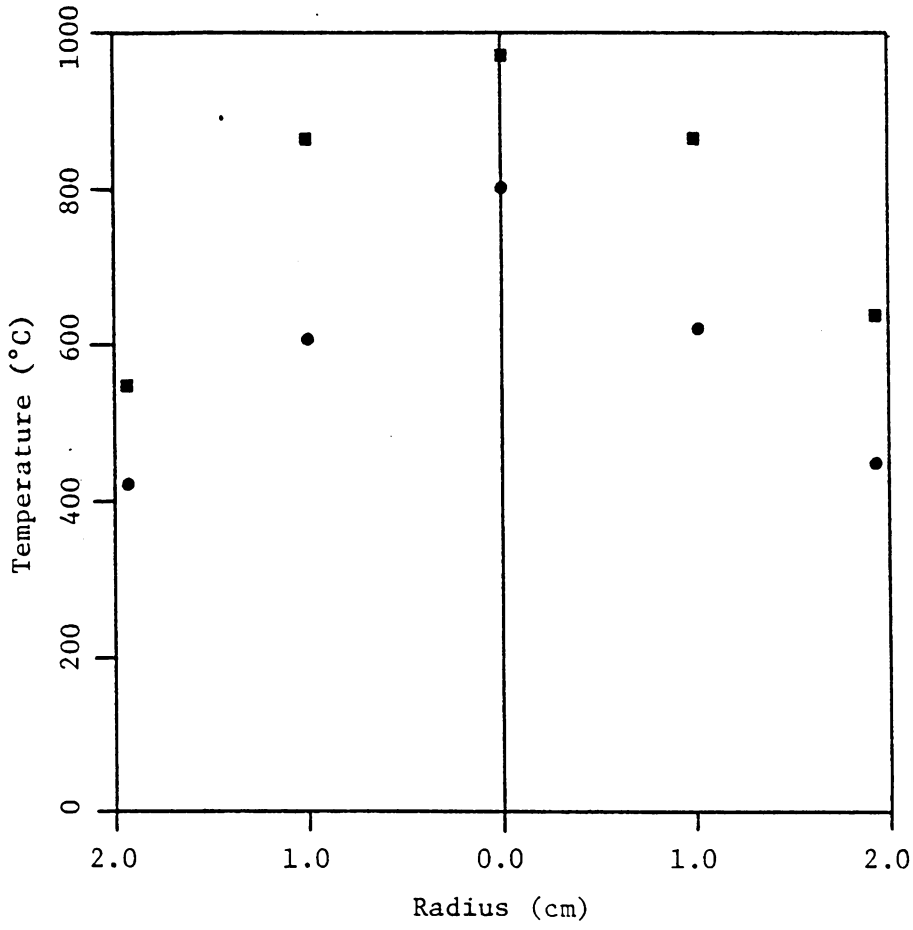

Figure 21. Radial Temperature Profiles for the Porous Disk Burner. Fuel is H_2, no radiation corrections, 0.075 mm thermocouple wire

for spectroscopic examination.

A second flame was created with the rectangular (5 cm X 25 cm) burner. The flame was viewed along the direction of the long side of the burner through quartz observation windows. The flame appeared with a visible reaction zone about 1 or 2 mm thick, but again significant flame curvature existed along the long axis and the narrow axis of the burner. Natural convection did not allow a really flat flame. The above conclusions are supported by the horizontal temperature profiles at various stations along the porous plate, as shown in Fig. 22. The temperature gradients along the optical axis are not as great as before, but once more they are not acceptable for spectroscopic measurements.

The last combustor assembly created an opposed-jet flame. There are some differences between the opposed type flame of the last burner and the other burners. The flame is again out of contact of any wall, but it is possible to vary the ratio of fuel to air and so obtain effects rather similar to those of changing the mixture strength, although the burner produces a diffusion flame. The opposed jet burner allows a long optical path and gives the opportunity to seed the flame (air supply) with known amounts of NO without producing any temperature or concentration gradients along the optical path and without destroying the structure of the flame. For reasons discussed later the flame must be seeded with 95 ppm of nitric oxide. The effects at the burner's rim were reduced by forced convection from the lower porous plate, and a flat rectangular-shaped flame was produced between the plates. The constant thickness of the visible reaction zone was less than 1 mm and

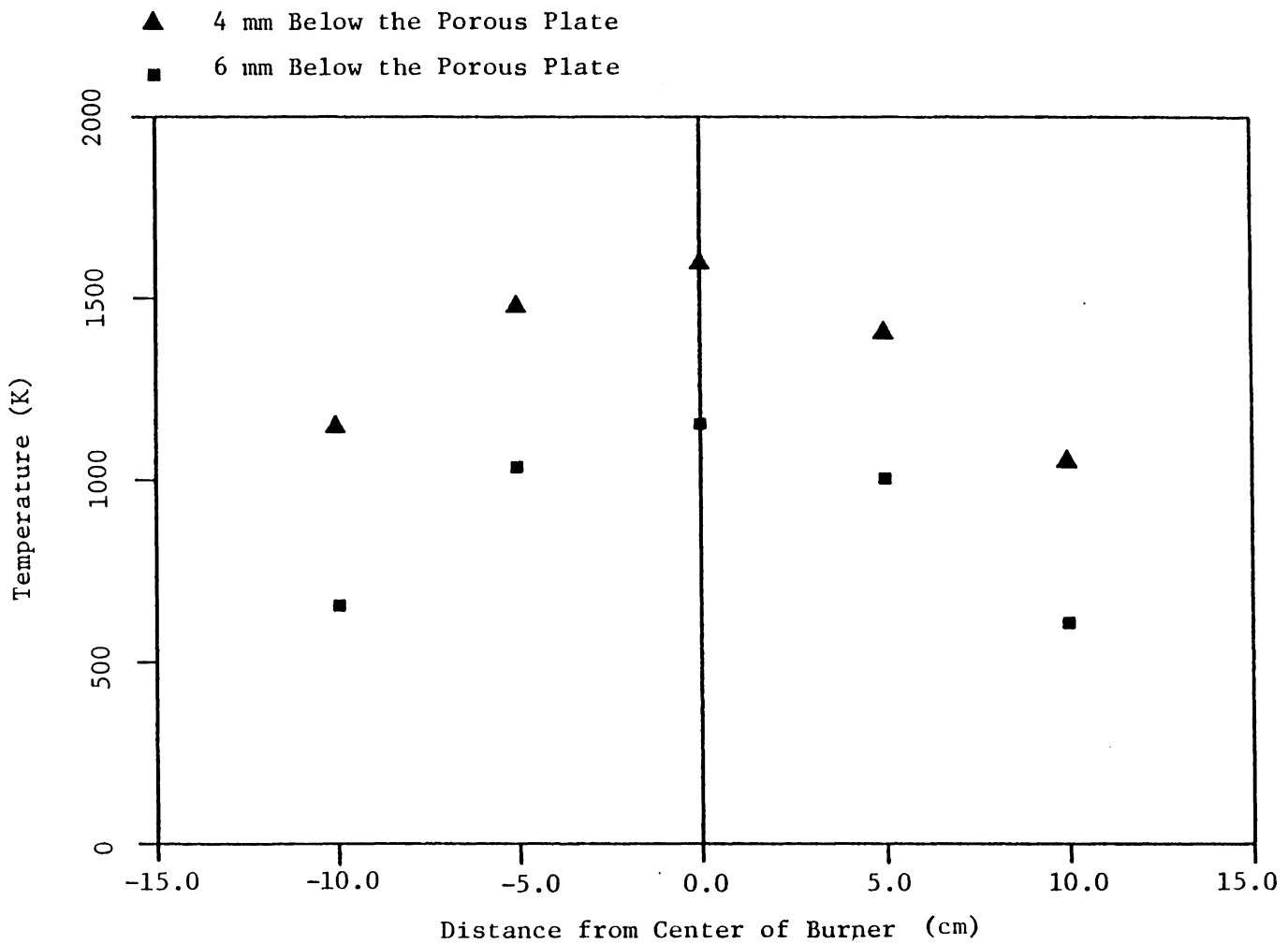

Figure 22. Horizontal Temperature Profiles Along the Major Axis of the Rectangular Burner. No radiation corrections, 0.075 mm thermocouple wire.

was located about 4 mm below the upper porous plate. Figure 23 gives the vertical temperature profile for these conditions while Fig. 24 shows some of the measured horizontal (along the long axis) temperature profiles at various positions above, inside, and under the visible reaction zone. The results of this work show that the flame was reasonably one-dimensional for much of the burner length.

An energy balance for the unshielded spherical junction of the thermocouple was performed assuming the Nusselt number is two. Using a 0.05 mm bead diameter the temperature error due to radiation heat losses is less than 50 K for the highest bead temperature (1650 K) assuming emissivity of unity. Thus the temperature correction is unnecessary causing at most 2% error in spectroscopically measured NO concentration.

During the spectroscopic measurements the air supply was doped with various concentrations of CH_4, but the flow rates and flame structure were negligibly changed.

The fuel flow rate is 1.2 l/min for all the following work. The above-described flame is very suitable for detailed spectroscopic examination of its structure.

5.4 Calibration Results

Figure 25 shows the spectral energy in Volts as a function of wavelength for different concentrations of nitric oxide with a monochromator bandpass of 0.16 nm. A strong absorption of spectral energy is observed due to the (0,0) gamma band of NO at 226.2 nm and an even

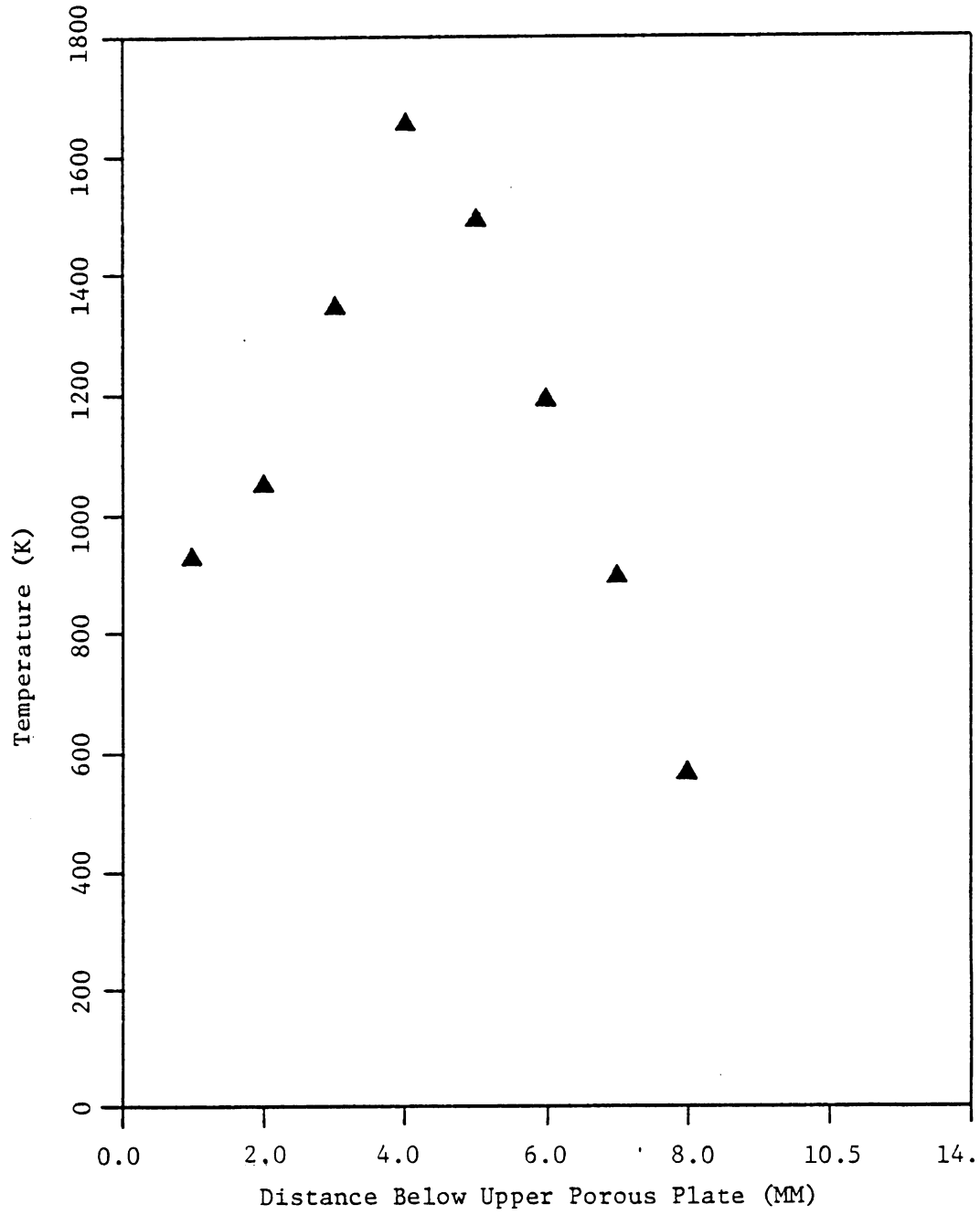

Figure 23. Vertical Temperature Profile for Opposed Jet H_2-Air Diffusion Flame. No radiation corrections, 0.025 mm thermocouple wire.

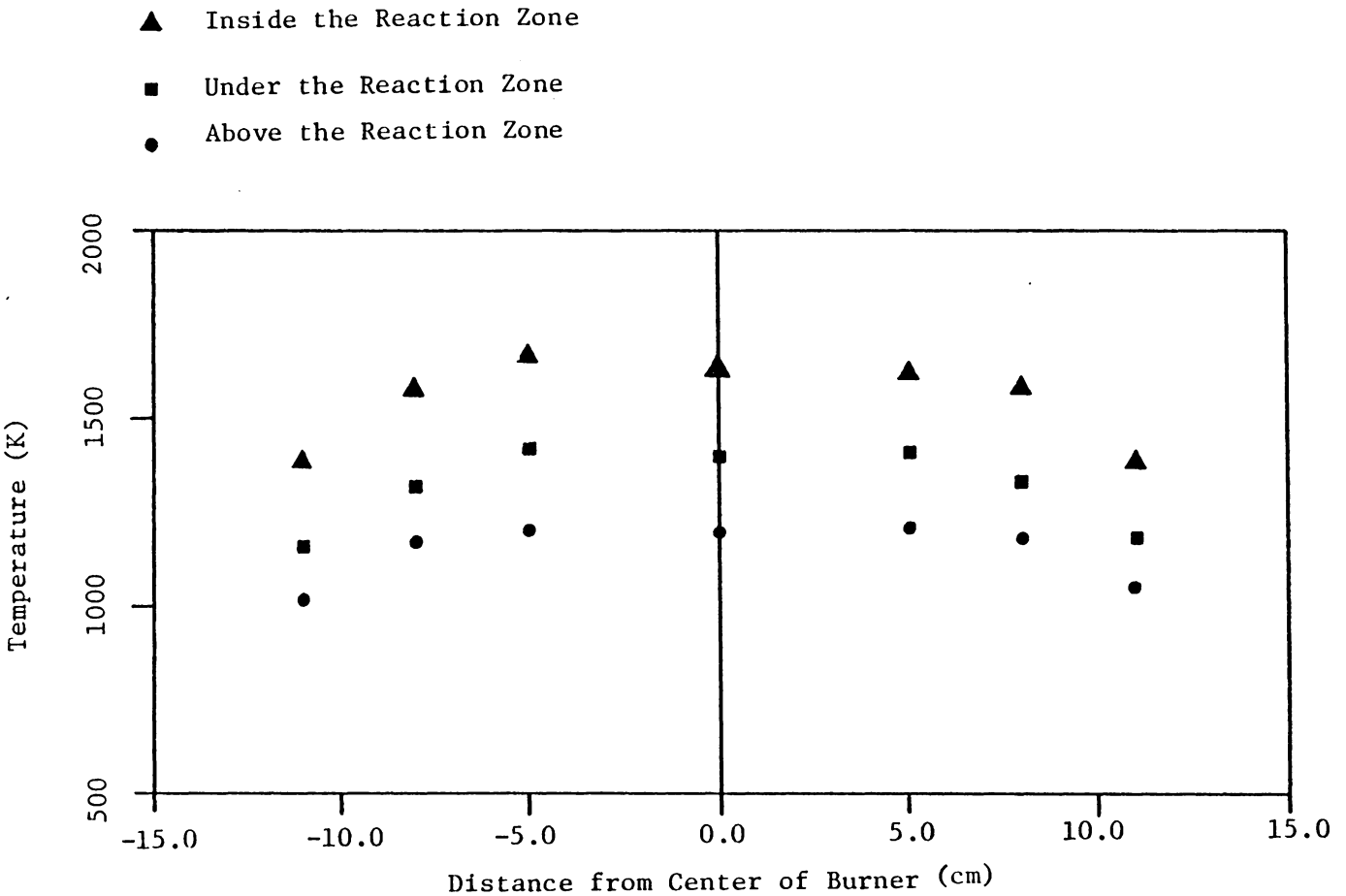

Figure 24. Horizontal Temperature Profiles Along the Major Axis of the Opposed Jet Burner. No radiation corrections, 0.025 mm thermocouple wire.

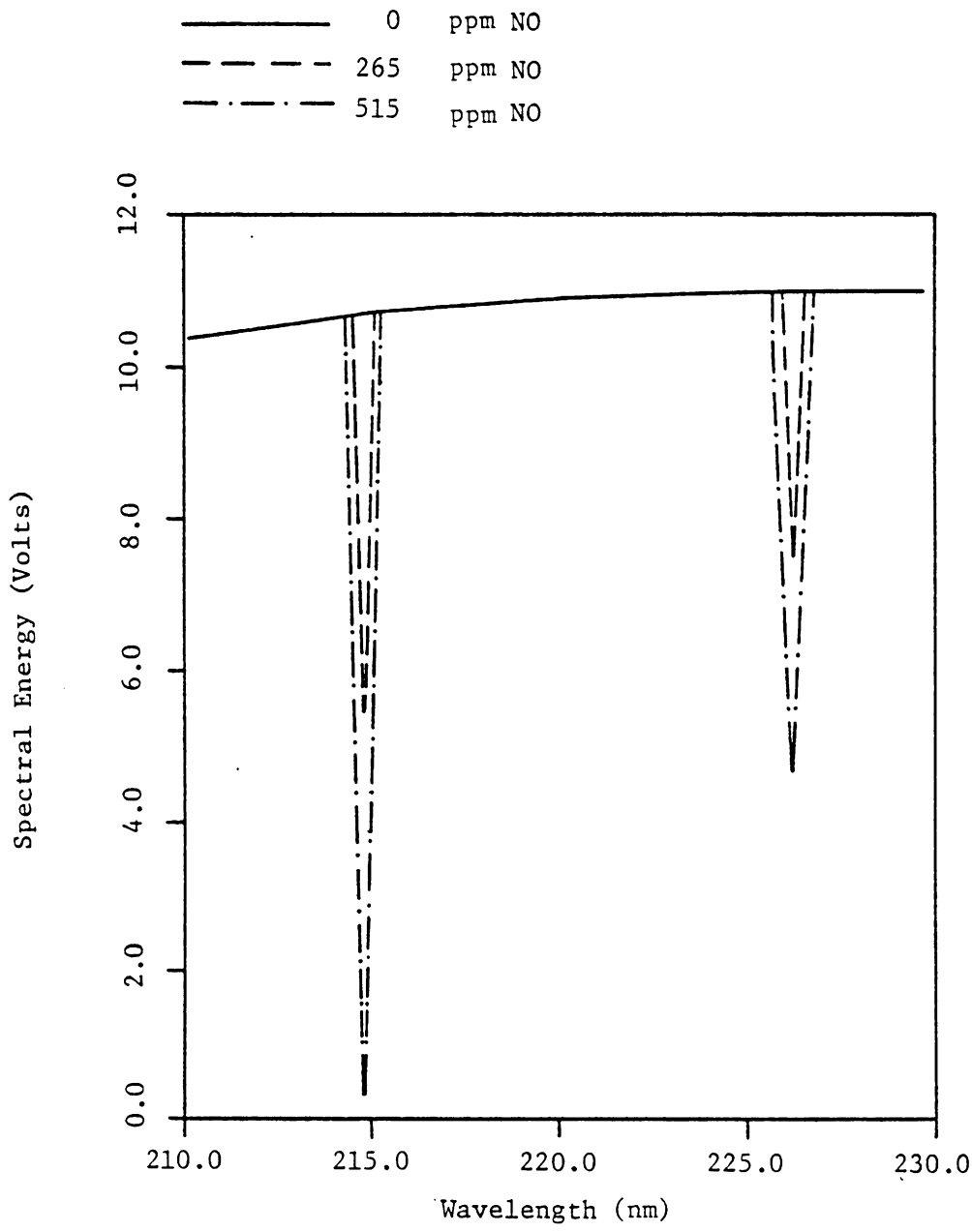

Figure 25. Spectral Energy Absorption. Monochromator Slit Width 0.1 mm, room temperature, optical path length 32 cm.

stronger absorption due to the (1,0) gamma band at 214.8 nm. As anticipated, the absorption is greater as the concentration of nitric oxide increases.

The percent spectral absorption, A_λ, is plotted for wavelengths of 226.2 nm and 214.8 nm in Fig. 26 as a function of nitric oxide concentration, with a bandpass of 0.16 as a parameter, and in Fig. 27 as a function of bandpass (or slit width) with nitric oxide concentration of 124 ppm as a parameter. The per cent spectral absorption is greater at 214.8 nm than at 226.2 nm because the (1,0) bands have the strongest intensity of the system. For that reason the spectroscopic measurements were performed at 214.8 nm, even though it was obvious that the background absorption due to oxygen molecules would be stronger. Figure 27 shows that the spectrometer slit width is very important, especially if high resolution measurements are desired. A 0.1 mm width for both slits was used, which gave a bandpass of 0.16 nm and was maintained constant throughout calibration and experimental runs. It is obvious that an even higher resolution is always desirable but the energy of the ultraviolet radiation which strikes the grating of the monochromator drops rapidly as the width of the slits is decreased.

The experimental data for the per cent spectral absorption was used in conjunction with the expression

$$K_\lambda = -\ln(1-A_\lambda)/C_{NO}L$$

to obtain the spectral absorption coefficent K_λ, which is shown in Fig. 28 as a function of nitric oxide concentration for the selected

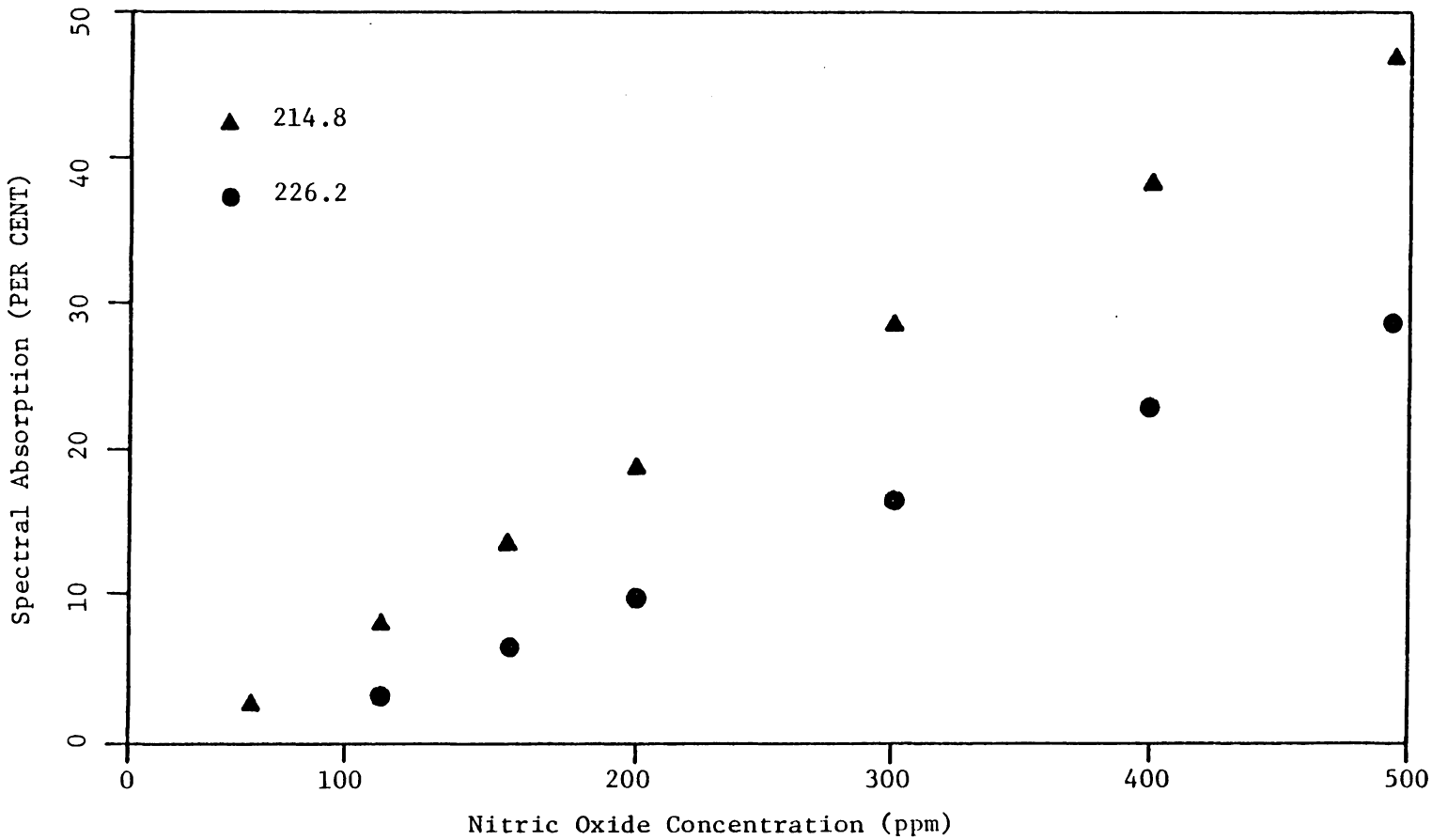

Figure 26. Per cent Spectral Absorption. Monochromator slit width 0.1 mm, room temperature, optical path length 25 cm.

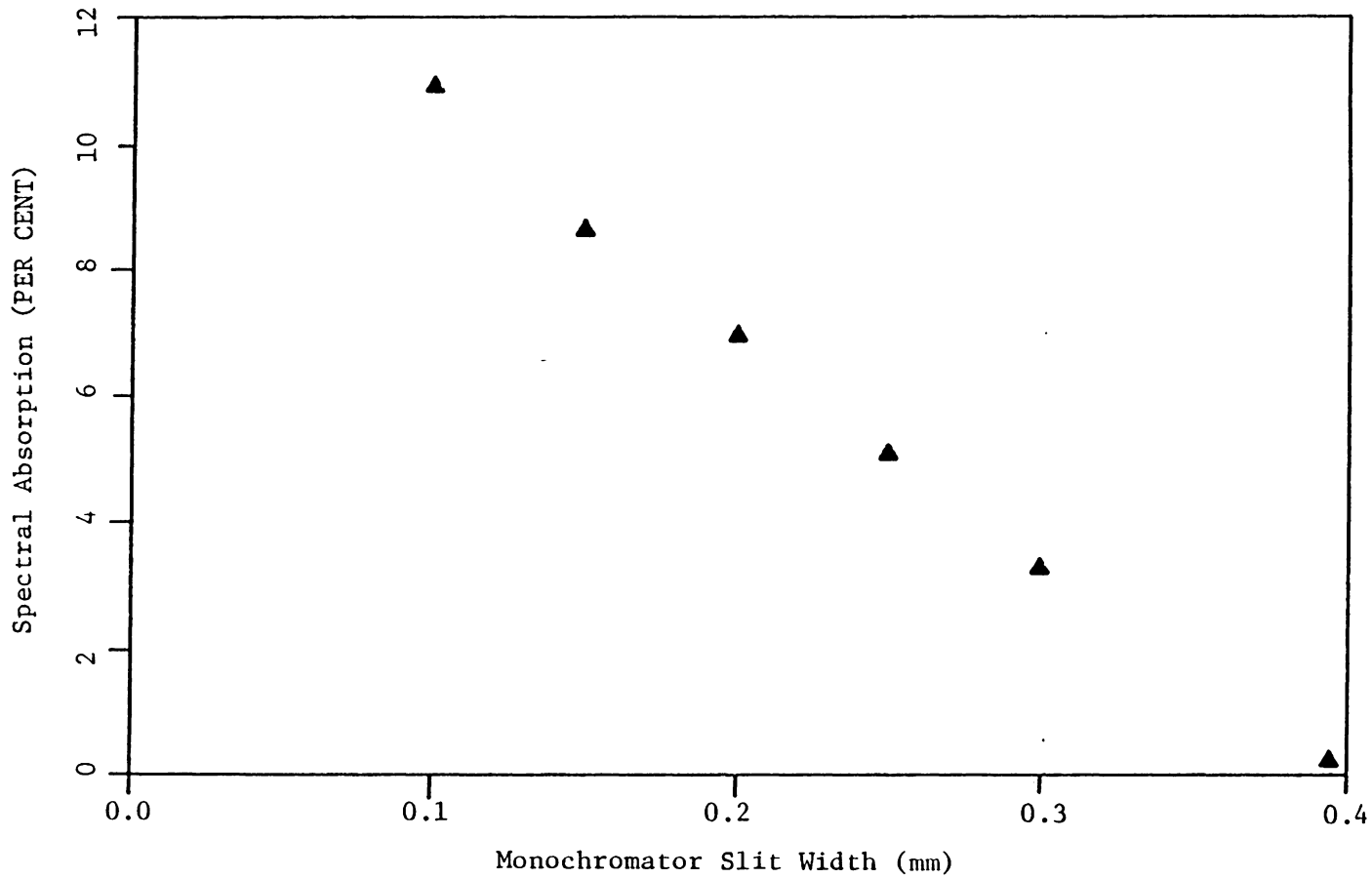

Figure 27. Per cent Spectral Absorption. Nitric oxide concentration 124 ppm, room temperature, optical path length 25 cm.

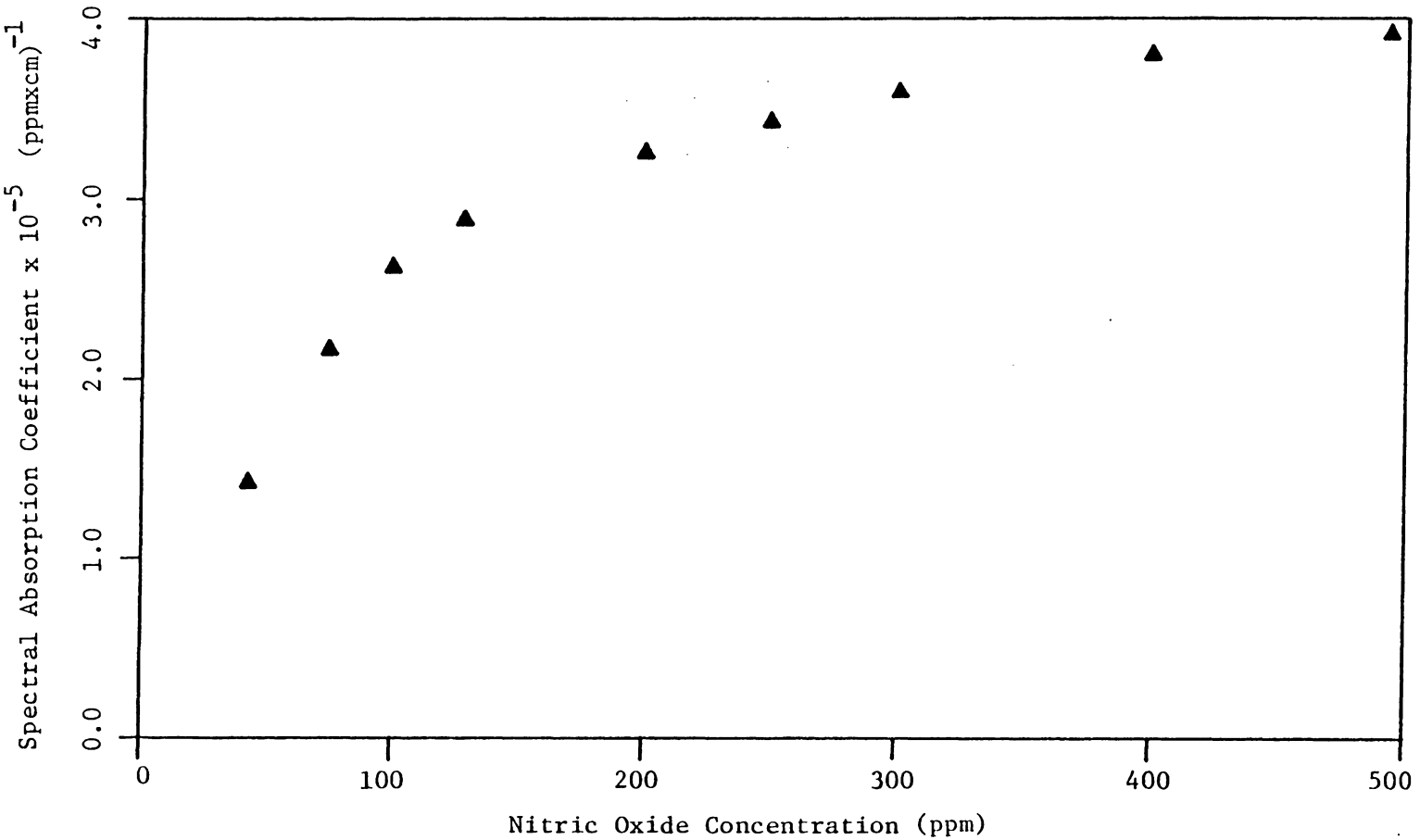

Figure 28. Spectral Absorption Coefficient. Monochromator slit width 0.1 mm, monochromator counter at 214.8 nm.

bandpass of 0.16 nm at 214.8 nm. A temperature correction based on the equilibrium depopulation of the ground vibrational state at flame temperatures is applied to the calibration results.

5.5 Porous Sphere Flame

Figure 29 shows the downstream concentration of NO_x and NO as a function of hydrogen concentration in the air around the flame. A very small decrease of NO_x concentration happens while the concentration of NO drops rapidly to very low levels when the air is doped with hydrogen. The break-down of hydrogen in the high temperature region and its oxidation outside the flame envelope will produce species such as OH and HO_2, which in turn could oxidize the NO molecules to NO_2. Previous work by Jaasma and Borman (2) showed that the presence of hydrocarbons in the air around such a flame causes conversion of NO to NO_2, but left open the question of whether a carbon-containing dopant was a necessary part of the mechanism. The present results show that the NO to NO_2 mechanism involves only radicals formed during H_2 oxidation.

5.6 Flat Plate Burner Flame

5.6.1 Spectroscopic Measurements of NO

The opposed jet burner was used to perform spectroscopic measurements of NO because, of the burners tested, it provided the most one-dimensional flame. Although a relatively long optical path (0.25 m) was

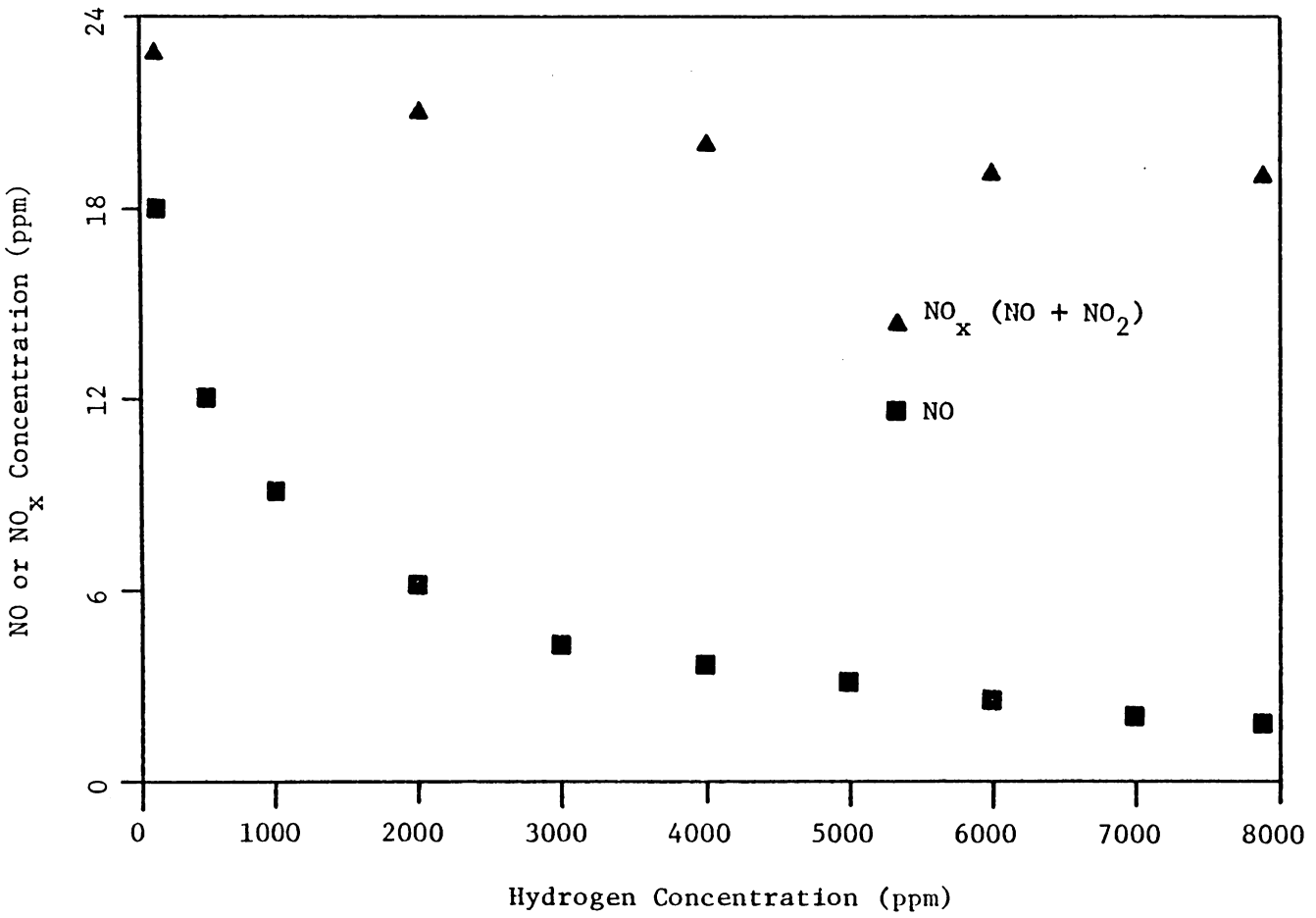

Figure 29. NO_2 Production for Diffusion Flame Around Porous Sphere Burning in Air Doped with H_2.

used, the flame's low concentrations of NO and the high temperatures in the flame zone did not permit a measurable NO-caused absorption at 214.8 or 226.2 nm. Several modifications of the optical system, such as higher resolution and improved focussing, were tried without success. To insure significant optical absorption, the air side of the flame was seeded with NO. The seed level was 95 ppm for all tests involving spectroscopic measurements.

As explained in the previous chapters, the optical system allowed measurements of NO between the two porous plates at any desired elevation. The nitric oxide concentration measurement for one position was immediately followed by measurement of background absorption. The relative levels of background and nitric oxide absorption for one position are illustrated in Fig. 30. The measured gamma band absorption due to nitric oxide is superimposed on the measured background absoprtion curve. During experimental runs, data similar to those plotted in Fig. 30 were obtained for each position of the optical path with respect to the flame. It was therefore possible to correct all recorded results for background absorption. A series of typical measurements of this background absorption at 214.8 nm is plotted in Fig. 31 as a function of the distance between the two porous plates.

The nitric oxide concentration profile via spectroscopic measurements of the opposed jet flame burner is shown in Fig. 32. The concentration of NO is constant between the air plenum and the flame zone, and drops rapidly inside and just after the reaction zone. A peak in NO concentration was not observed just outside the visible flame zone,

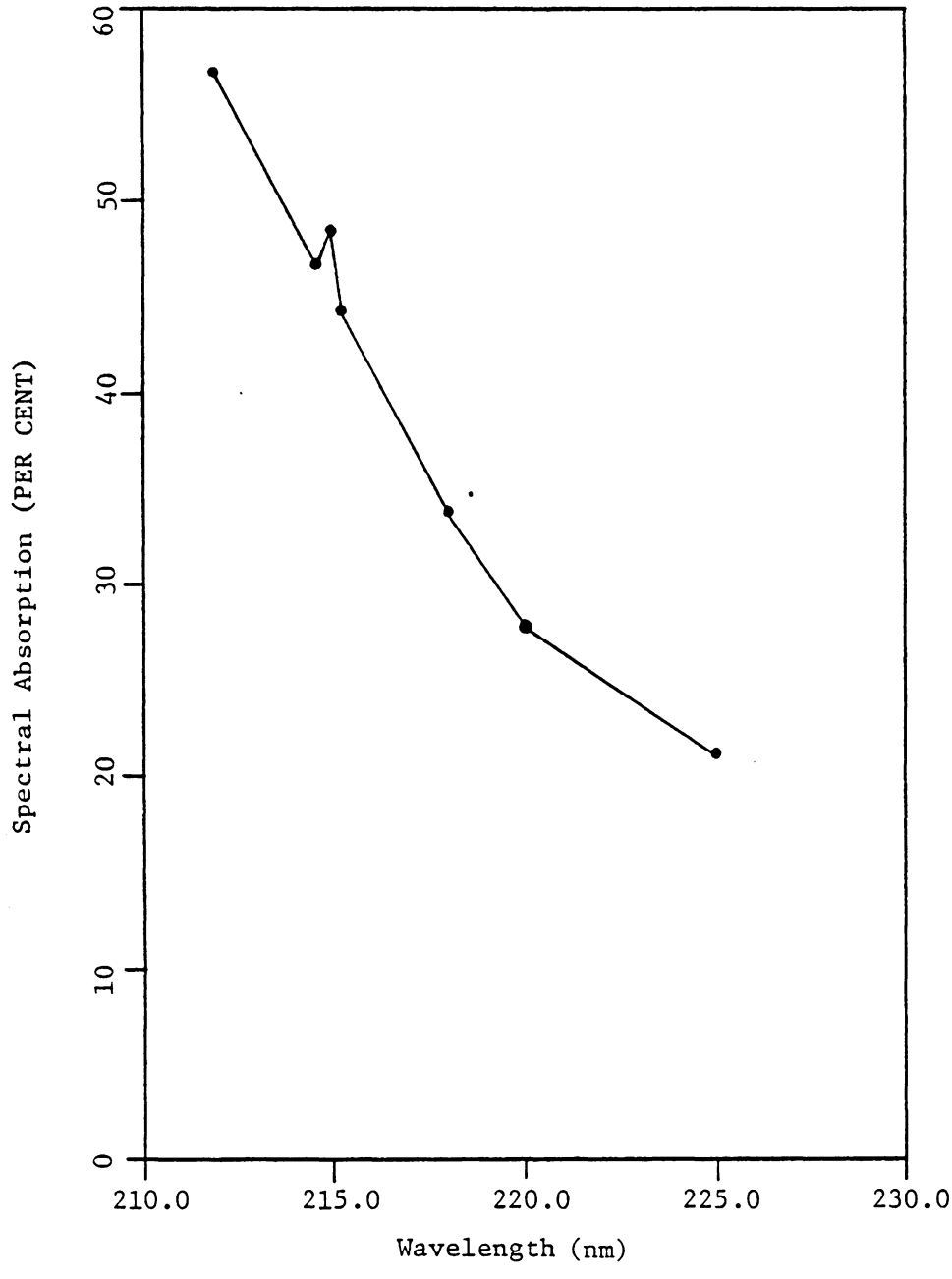

Figure 30. (1,0) Gamma Band of NO Absorption Superimposed on Background Absorption. Monochromator slit width 0.1 mm, 6 mm below the upper porous plate.

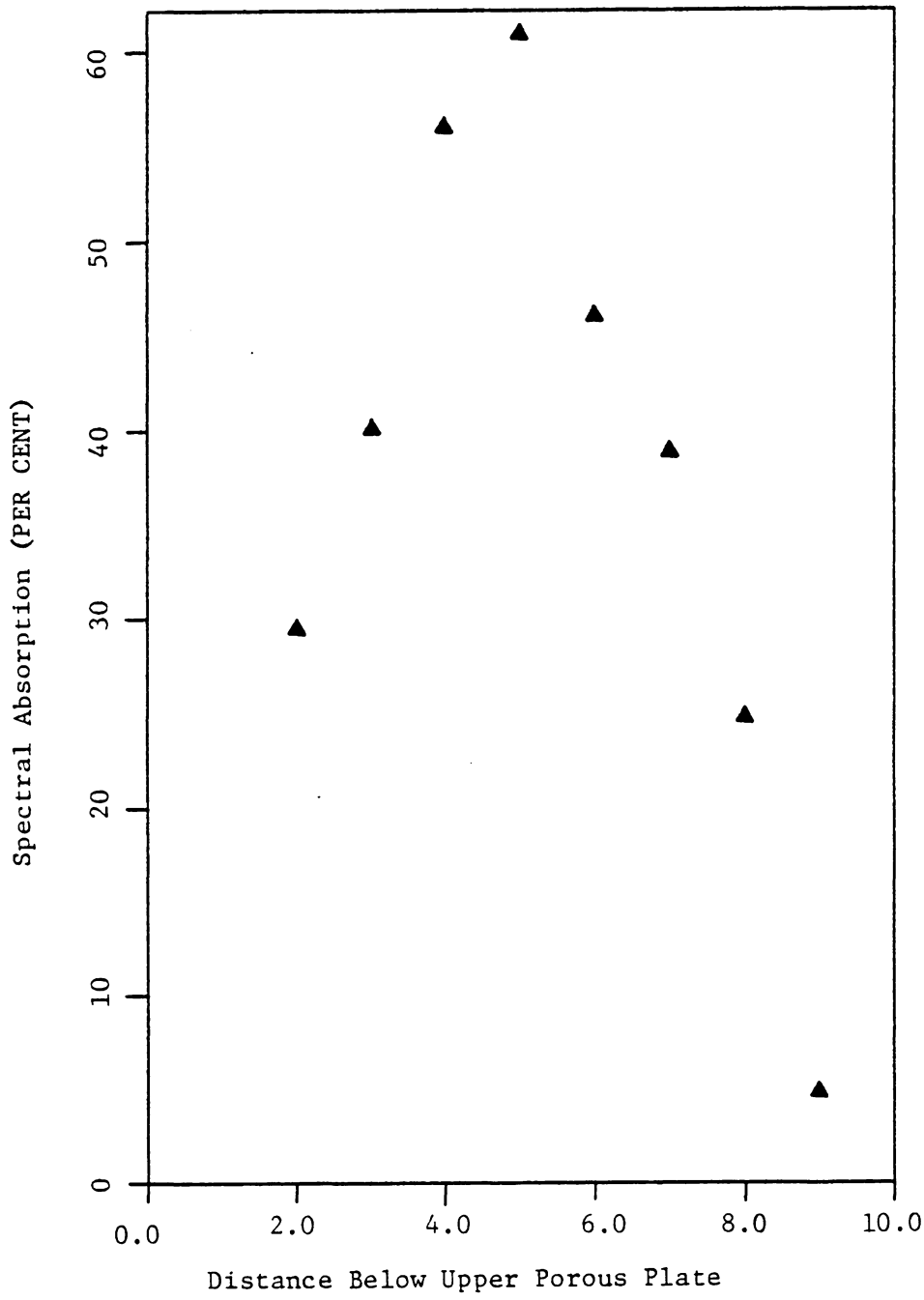

Figure 31. Background Absorption at 214.8 nm Monochromator Slit Width 0.1 mm

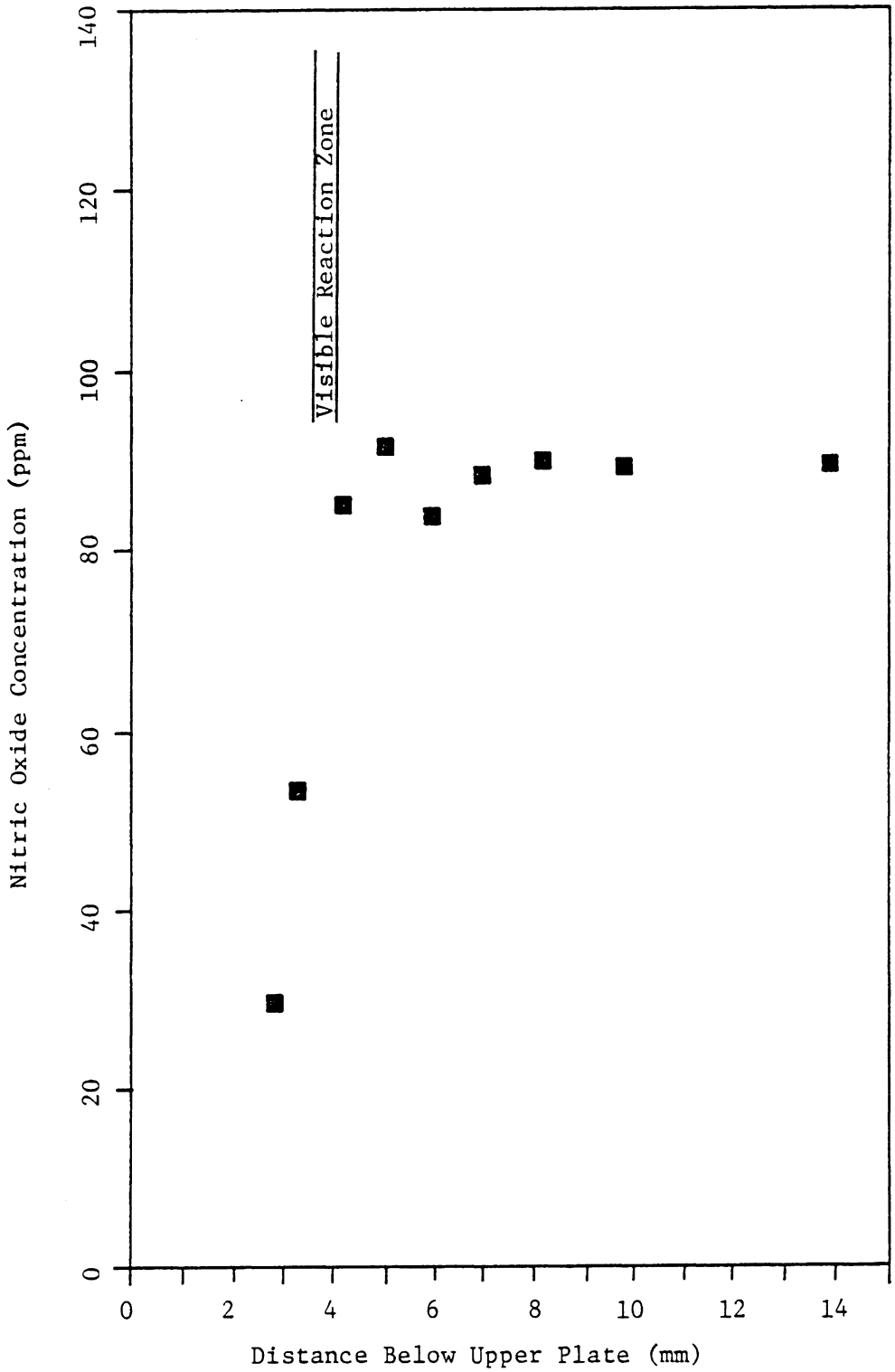

Figure 32. Spectroscopically Measured NO Profile of the Opposed Jet H_2-Air Diffusion Flame. Air stream seeded with 95 ppm NO

although such a peak was anticipated. The optical absorption decreases rapidly as the path moves upward through the flame, and it is not possible to tell whether this is because NO can not diffuse against the fuel flow or is being converted to NO_2 due to an abundant presence of OH and HO_2. The spectroscopically measured concentration of NO near the air plenum was 90 ppm, while using a probe above the porous plate gave a probe-measured concentration of 95 ppm. The author believes this to be excellent agreement.

Figure 33 illustrates the NO concentration at one elevation (5 mm below the fuel plenum) of the optical beam while the air side of the flame was doped with different amounts of CH_4.

At this position, the concentration of NO when the air is not doped with methane is 93 ppm. As shown, the increase of the unburned hydrocarbon concentration has a significant effect on the probe-measured concentration of NO. Only about 1000 ppm of CH_4 is required to reduce the NO concentration by a factor of two. When the concentration of CH_4 is over 1500 ppm the per cent optical absorption is not adequate to allow further measurements. For that reason a concentration of 1200 ppm for CH_4 was selected and maintained constant for the next experimental runs.

The concentration profile of nitric oxide is illustrated in Fig. 34 for the case when the air of the flame was doped with 1200 ppm CH_4 and the non-CH_4 doped profile from Fig. 32 is plotted for reference. Near the air the concentration of nitric oxide remained at the seed level. About 3 mm from the reaction zone a decrease of NO concentration is noticed which becomes stronger as the optical beam is moved nearer

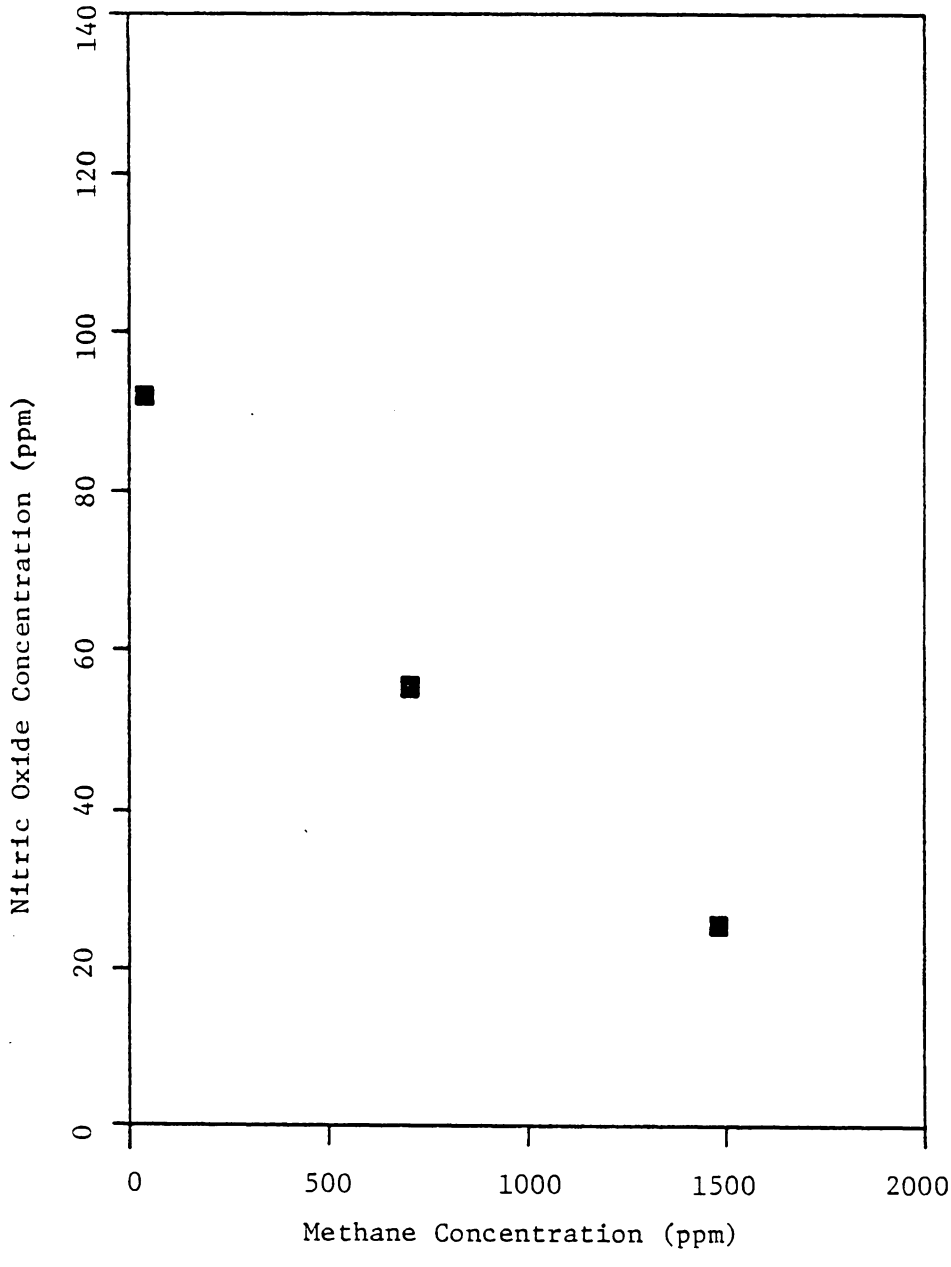

Figure 33. Spectroscopically Measured NO Profile at 5 mm Below the Upper Porous Plate of the Opposed Jet H_2-Air Diffusion Flame. Air stream seeded with 95 ppm NO and doped with CH_4

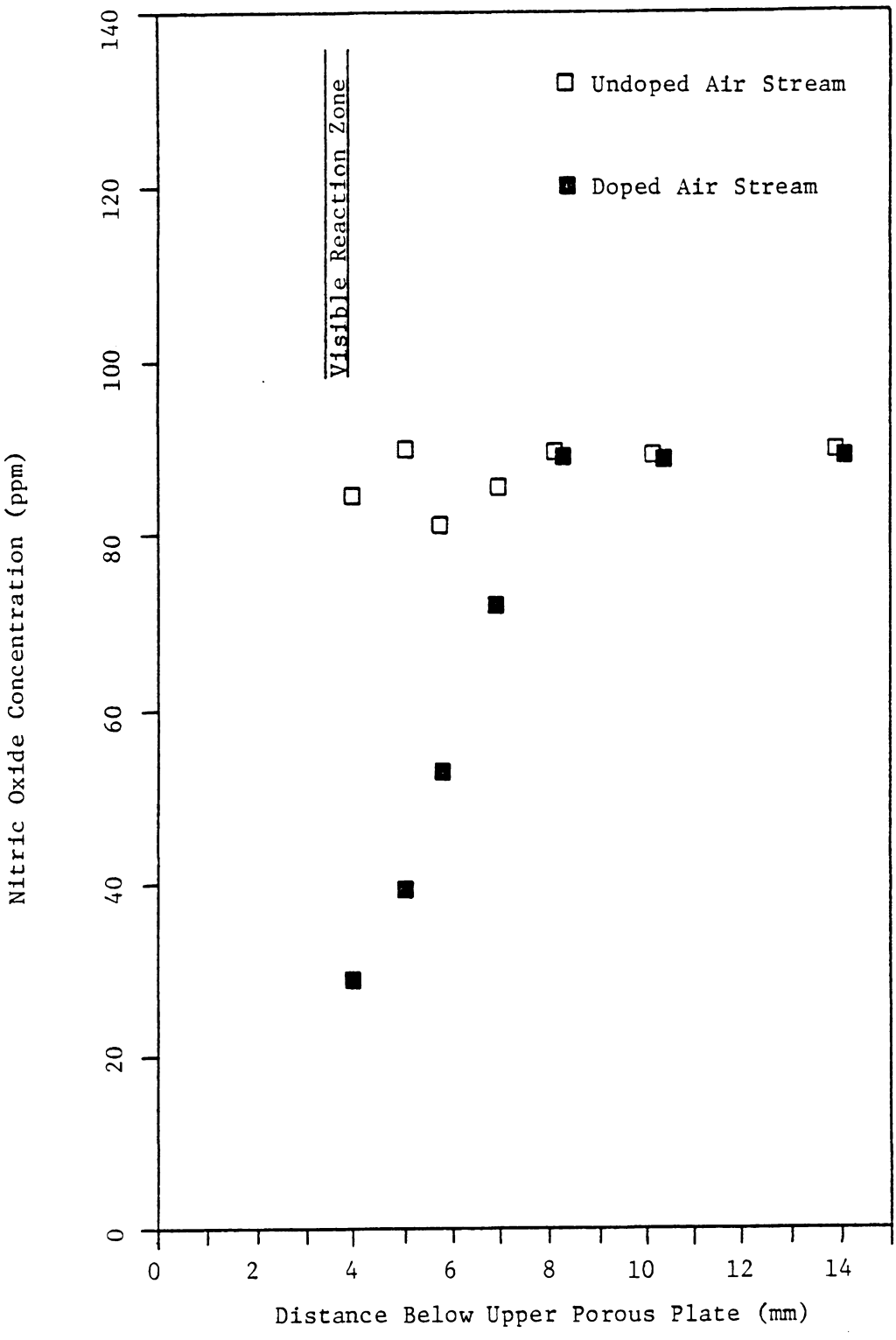

Figure 34. Spectroscopically Measured NO Profile of the Opposed Jet H_2-Air Diffusion Flame. Air stream seeded with 95 ppm NO and doped with 1200 ppm CH_4.

the visible reaction zone where the high temperature zone exists. The spectroscopic measurements stop inside the reaction zone where the nitric oxide concentration is already very low. From this it is concluded that the destruction of NO starts about 3 mm below the flame and the concentration of NO is eliminated rapidly in front of the reaction zone.

5.6.2 Probe Sampling for NO

Figure 35 shows the vertical (at plate center) concentration profile of NO for the opposed jet flame burner and Fig. 36 shows some horizontal profiles at various elevations along the optical path while the flame is not seeded with additional nitric oxide. There are no significant concentration gradients across the narrow dimension of the plate. The vertical concentration profile of NO show a peak at 22 ppm.

The concentration profile of NO for the opposed jet burner with 95 ppm seeded NO is shown in Fig. 37. Horizontal measurements of NO concentration at different elevations which are shown in Fig. 38 confirm the assumption of a one-dimensional flame. The concentration of NO is 95 ppm above the air plenum and gradually increases until the visible reaction zone. The concentration of NO is constant near the air plenum, has a maximum value under the visible reaction zone, and drops inside and after the reaction zone. The NO concentration profile for the case when the air of the flame is doped with 1200 ppm methane is shown in Fig. 39. Once more the free stream unburned hydrocarbon concentration has a dramatic effect on the measure NO profile. The concentration of

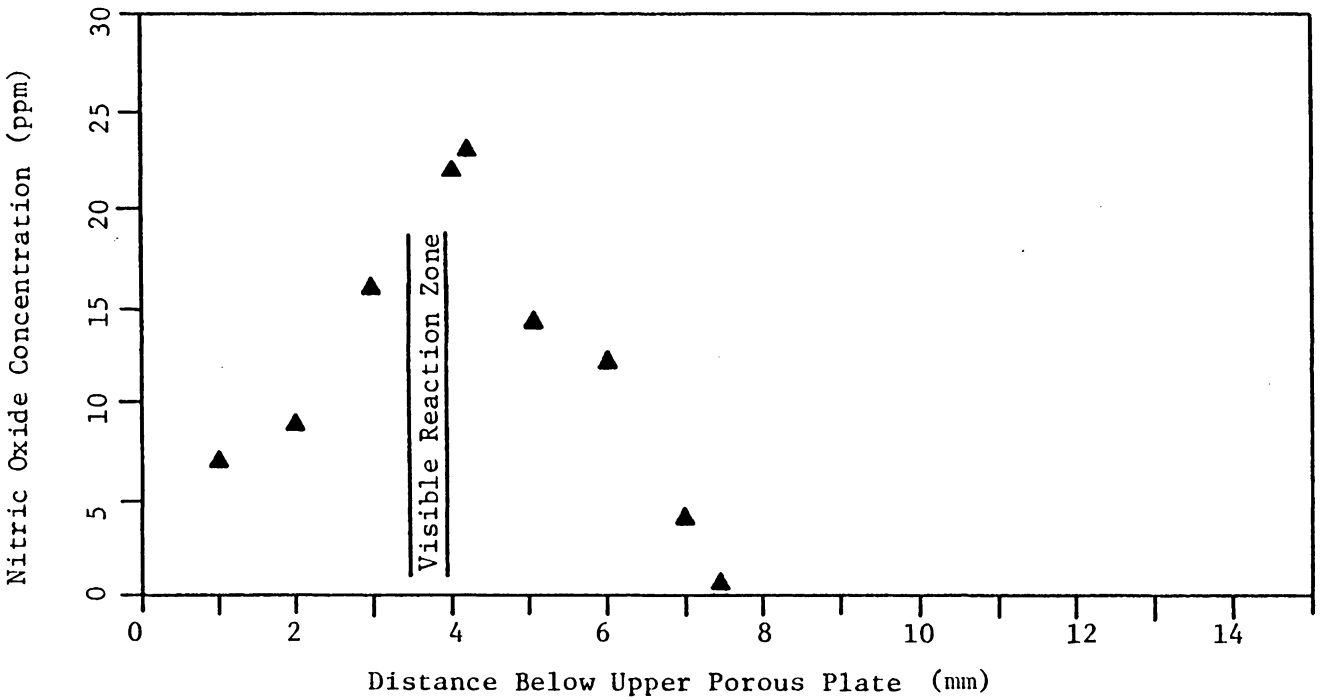

Figure 35. Probe Measured NO Profile of the Opposed Jet H_2-Air Diffusion Flame

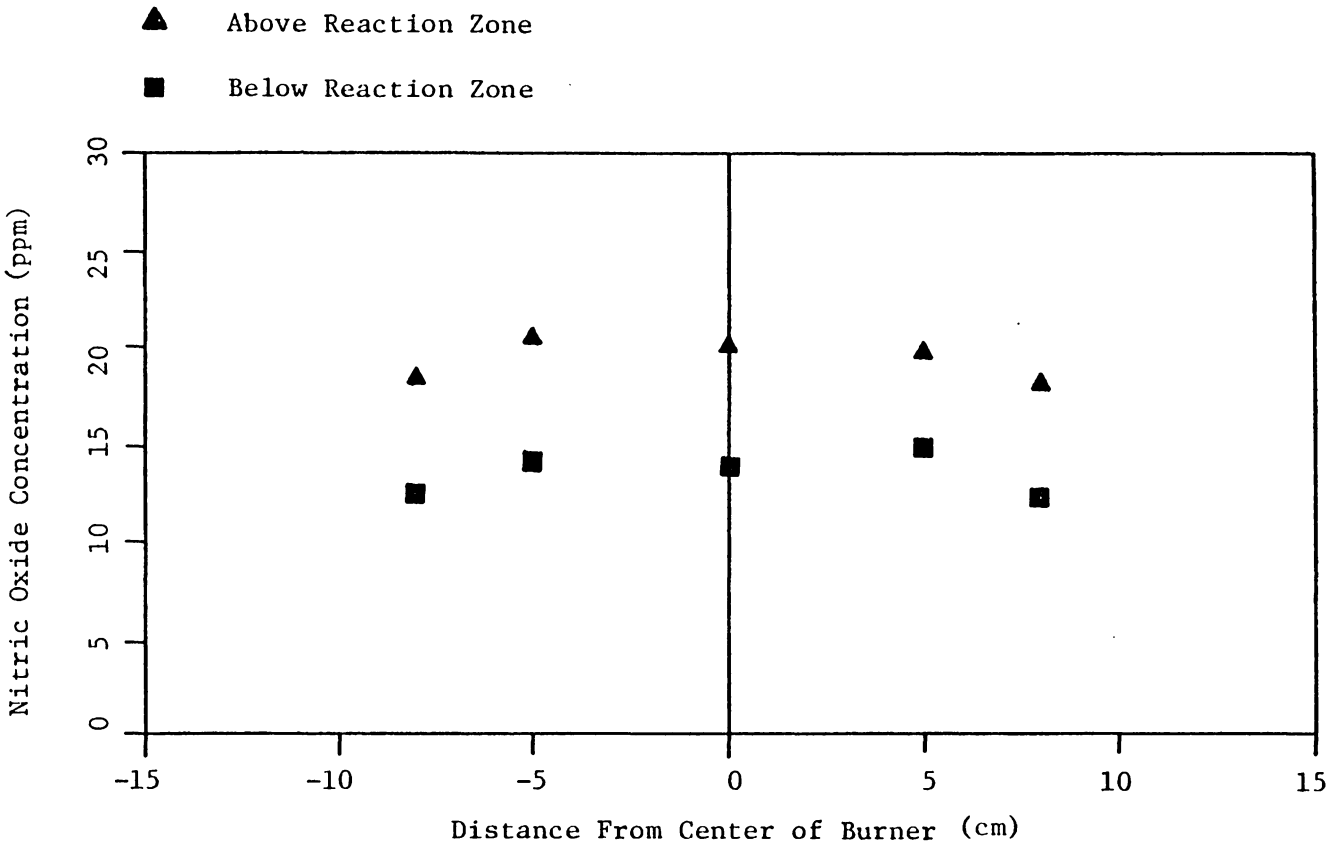

Figure 36. Probe Measured NO Profiles Along the Major Axis of the Opposed Jet H_2-Air Diffusion Flame.

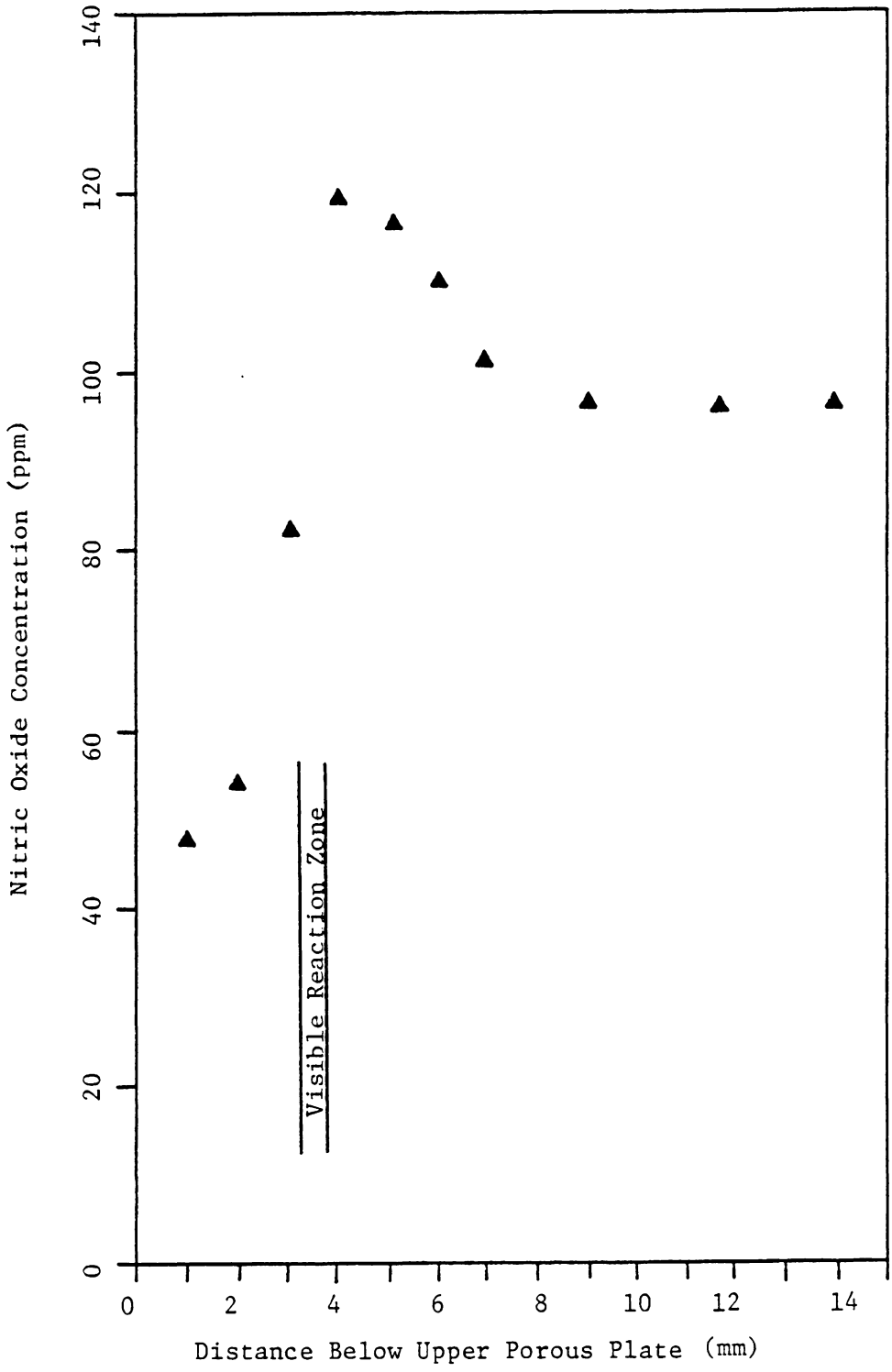

Figure 37. Probe Sampling NO Profile of the Opposed Jet H_2-Air Diffusion Flame. Air stream seeded with 95 ppm NO

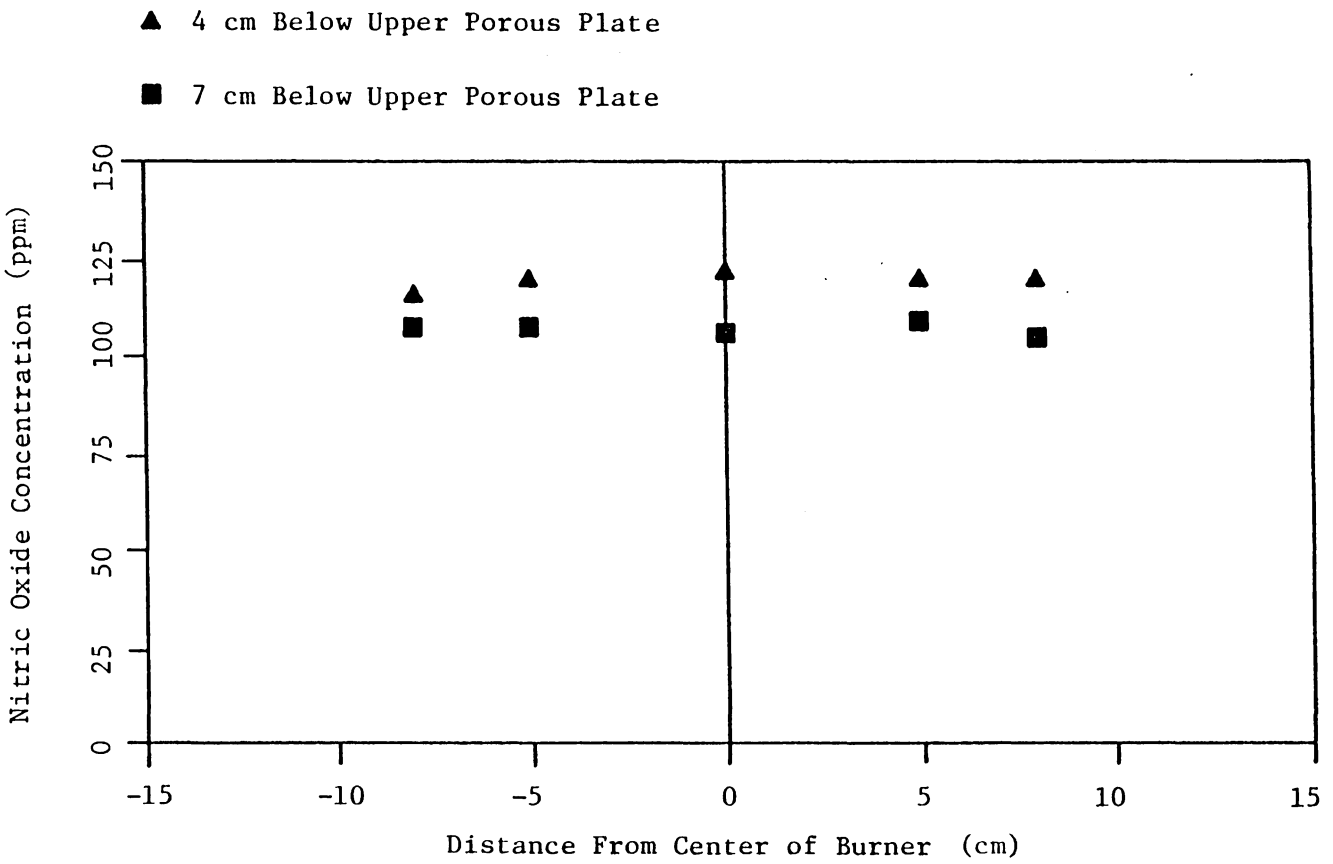

Figure 38. Probe-Measured NO Profiles Along the Major Axis of the Opposed Jet H_2-Air Diffusion Flame. Air stream seeded with 95 ppm NO.

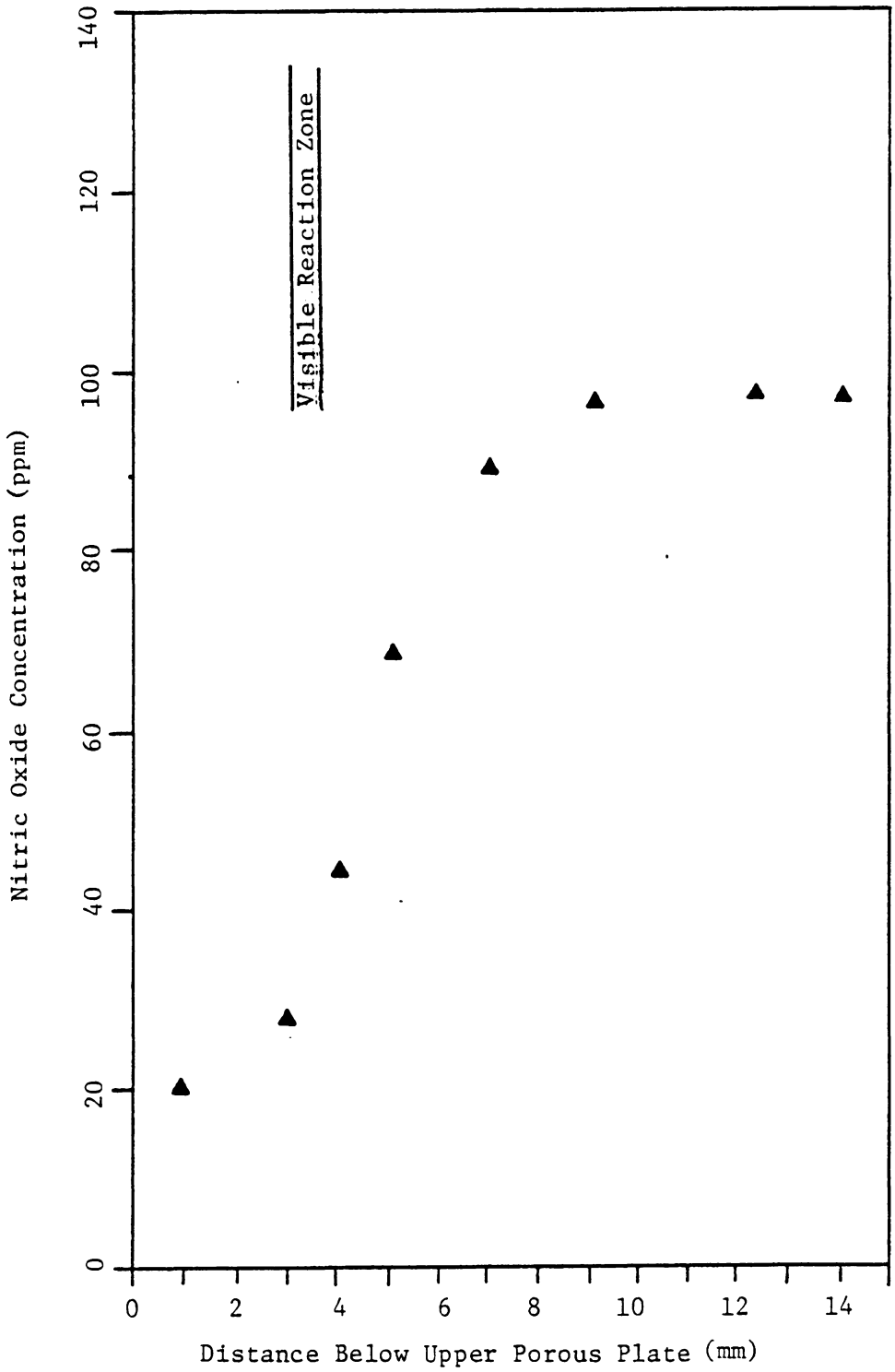

Figure 39. Probe Measured NO Profile of the Opposed Jet H_2-Air Diffusion Flame. Air stream seeded with 95 ppm NO and doped with 1200 ppm CH_4

NO drops about 60 per cent just outside the flame.

5.7 Summary

Three types of diffusion flames have been tried to evaluate their suitability for optical measurement of NO. After temperature and probe-measured nitric oxide concentrations were obtained for all three types of flame, the opposed jet burner was considered most appropriate for this type of measurement.

In Fig. 40 the probe and spectroscopic concentration profiles of NO for the undoped air and air doped with methane cases are plotted together and give important results. Both spectroscopic and probe measurements definitely confirm that NO is destroyed near the flame when the air of the flame is doped even with small concentrations of hydrocarbons. Taking into account that in the room temperature portion of the air flow the spectroscopic measurement of the air stream NO concentration was about 6 per cent low compared to the (presumably accurate) probe measurements (and could be corrected for), it is concluded that ultraviolet absorption concentration measurements are in agreement to within 30 per cent with probe-determined concentrations. For reasons unknown at this time probe measurements are higher. Finally, it is believed that the high measured probe concentration of NO in the above-flame region is due to the minimized ability of conventional methods to sample only one position in the flame. Operational difficulties with the NO_x analyzer did not allow measurements of NO and NO_2 concentrations

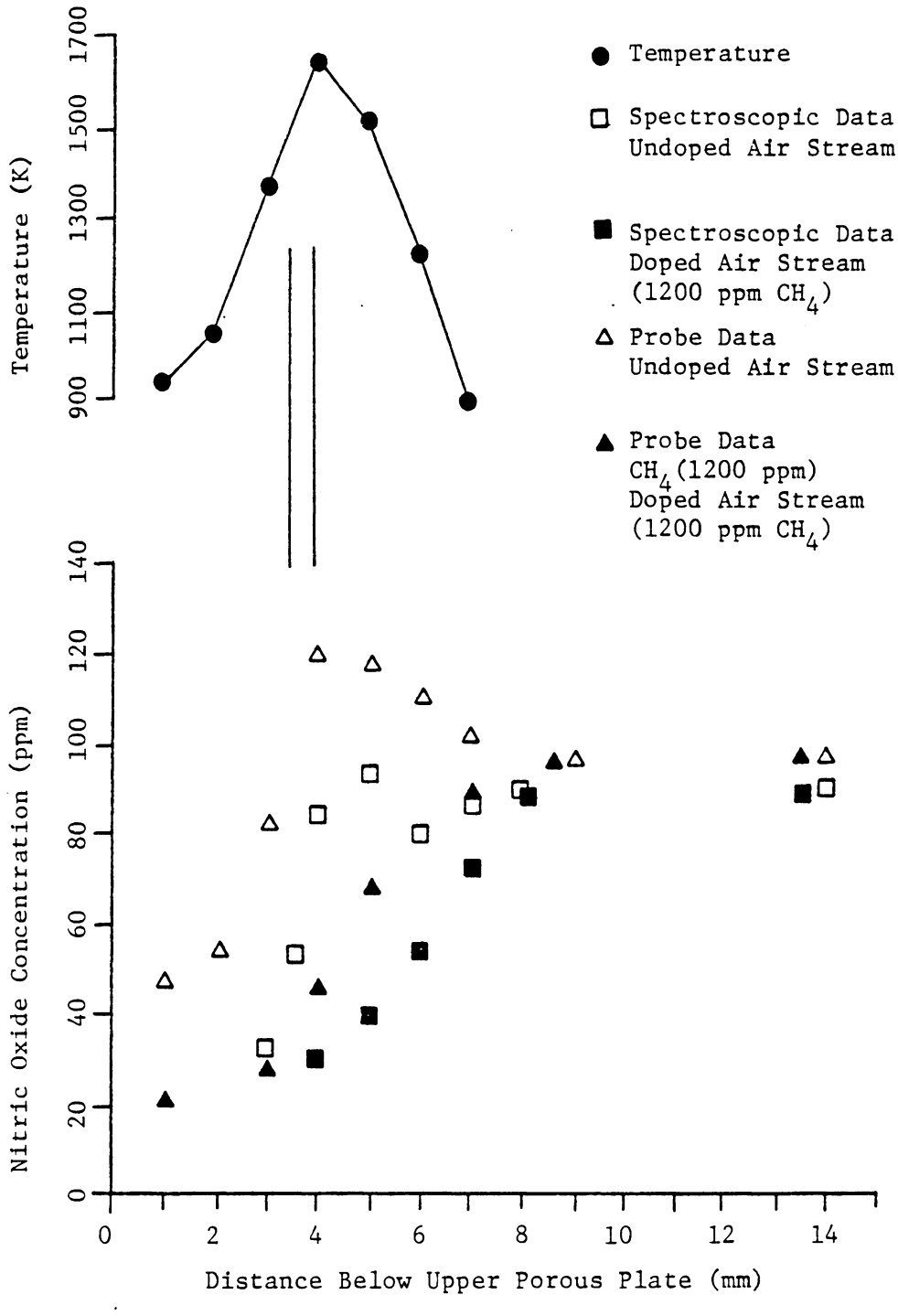

Figure 40. Superimposed Spectroscopic and Probe Measured NO Profiles of the Opposed Jet H_2-Air Diffusion Flame. Air stream seeded with 95 ppm NO

of the gases downstream of the opposed jet burner. Work with the spherical flame apparatus and the previous work of Jaasma and Borman confirm that the total number of moles of NO_x is being nearly conserved when the spherical flame's air stream is doped with hydrocarbons, and in these two cases NO is being converted to NO_2 on a mole for mole basis. The mixed products of the flat flame could have been sampled to determine if fixed nitrogen was conserved during doping of the air with CH_4, but this was not possible due to equipment failure.

VI. CONCLUSIONS

The conclusions of this research are:

1) Spatially resolved spectroscopic measurements of NO in a laminar H_2-air diffusion flame are possible provided the air stream is seeded with ca. 100 ppm NO.

2) Spectroscopic measurements of NO concentration confirm the disappearance of NO when the air of a laminar diffusion flame is doped with methane.

3) The methane's influence is felt outside the diffusion flame.

4) For the system studied, spectroscopic and probe measurements of NO agree to within 30 per cent.

5) Conventional measurements of post-flame NO and NO_2 concentrations confirm that NO is oxidized to NO_2 when the air of a flame around a heptane-wetted cotton ball is doped with hydrogen.

6) No carbon atoms are required in the dopant for the interchange of 5 above.

Since it was not proved that NO was converted to NO_2 for the case of the flat flame, it is only certain that NO was destroyed. However, it is strongly believed that NO is oxidized to NO_2 in accordance with the porous sphere experiment data, since the doping conditions for both experiments were similar. Some investigators have suggested NO to NO_2

conversion mechanisms which require species such as OH or OH_2, and this is in agreement with the results of the present work. The break-down of hydrogen or hydrocarbon species and their subsequent oxidation outside the flame envelope can produce HO_2 and OH, which in turn can scavenge the NO molecules near the peak temperature region.

The agreement between optical and probe methods was somewhat unexpected, since a large number of investigators report probe oxidation reactions of NO which do not allow even approximately correct measurements of NO. However, the results of this work are in agreement with recent studies (26) which do not show large discrepancies between spectroscopic and probe sampling techniques.

VII. RECOMMENDATIONS

This work provides a definite answer to the question of where nitric oxide is scavenged when the air of a diffusion flame is doped with a hydrocarbon, but most of the problem areas associated with sampling and analyzing for NO and NO_2 require further work before the problems can be isolated, the effects fully understood, and appropriate corrections developed. The present experimental apparatus provides a powerful tool for flame spectroscopy. The following recommendations are presented:

1) An attempt should be made to perform spectroscopic measurements of NO in a diffusion flame without any seeded NO. The only way to improve the sensitivity of the molecular absorption with the same optical system is to increase the optical path. A new flat or curved burner which allows a longer optical path can be used, but a better solution to this problem might be to pass the light beam several times through the flame, using mirrors angled to counteract beam curvature. A three-pass system would probably allow direct measurement of NO concentration.

2) With a multipass system which allows the light beam to travel about ten times through the flame, direct spectroscopic measurement of nitrogen dioxide can be obtained in the vicinity of 448 nm. A different light source is required, but the conclusions of this work would be validated; the concentrations

for both nitric oxide and nitrogen dioxide could be measured in-situ and an effective comparison with probe data could be made.

3) Detailed kinetic modeling of a H_2-air diffusion flame should be used to model the concentration and temperature profiles of the flame and to try and verify the mechanism by which NO is converted to NO_2.

VIII. REFERENCES

1. Zeldovich, Y. B., "Acta Physicochim," URSS, 1946.

2. Jaasma, D. R., and G. L. Borman, "Peculiarities Associated with Measurement of Oxides of Nitrogen Produced by Diffusion Flames," Combustion Science and Technology, Vol. 23, n 1 and 2, 1980.

3. Allen, J. D., "Probe Sampling of Oxides of Nitrogen from Flames," Combustion and Flame, Vol. 24, n 1, 1975.

4. Burke, S. P., and T. E. Schumann, "Diffusion Flames," Industr. Engg. Chem., Vol. 20, 1928, p. 998.

5. Barr, J., "Combustion in Vitiated Atmospheres. Some Preliminary Studies of Diffusion Flames," Fuel, Vol. 28, 1949.

6. Fendell, F. E., "Ignition and Extinction in Combustion of Initially Unmixed Reactants," The Journal of Fluid Mechanics, Vol. 21, 1965.

7. Fendell, F. E., "Combustion in Initially Unmixed Reactants for One-Step Reversible Chemical Kinetics," Astronautica Acta, Vol. 13, 1967, p. 183.

8. Chung, P. M., and V. D. Blankenship, "Equilibrium Structure of Thin Diffusion Flame Zone," Physics of Fluids, Vol. 9, 1966, p. 1569.

9. Clarke, J. F., "The Laminar Diffusion Flame in Oseen Flow: The Stoichiometric Burke-Schumann Flame and Frozen Flow," Proc. Roy. Soc., Vol. A296, 1967a.

10. Clarke, J. F., "The Laminar Diffusion Flame Behind a Blunt Body: A Constant Pressure Oseen-Flow Model," Journ. Inst. Maths. Applics., Vol. 3, 1967b.

11. Clarke, J. F., "On the Structure of a Hydrogen-Oxygen Diffusion Flame," Proc. Roy. Soc., Vol. A307, 1968.

12. Clarke, J. F., "Reaction-Broadening in a Hydrogen-Oxygen Diffusion Flame," Proc. Roy. Soc., A312, 1969.

13. Melvin A., J. B. Moss, and J. F. Clarke, "The Structure of a Reaction Broadened Diffusion Flame," Combustion Science and Technology, Vol. 4, 1971.

14. Fenimore, C. P., "Formation of Nitric Oxide in Premixed Hydrocarbon Flames," Thirteenth Symposium (In National) on Combustion, The Combustion Institute, Pittsburgh, PA, 1971.

15. Merryman, E. L., and A. Levy, "Nitrogen Oxide Formation in Flames: The Roles of NO_2 and Fuel Nitrogen," Fifteenth Symposium (International) on Combustion, The Combustion Institute, Pittsburgh, PA, 1975.

16. Fenimore, C. P., "The Ratio NO_2/NO in Fuel-Lean Flames," Combustion and Flame, Vol. 25, 1975.

17. Cernansky, N. P., and R. F. Sawyer, "NO and NO_2 Formation in a Turbulent Hydrocarbon/Air Diffusion Flame," Fifteenth Symposium (International) on Combustion, The Combustion Institute, Pittsburgh, PA, 1975.

18. Amin H., "Effect of Heterogeneous Removal of Oxygen Atoms on Measurement of Nitrogen Dioxide in Combustion Gas Sampling Probes," Combustion Science and Technology, Vol. 15, 1977.

19. Cernansky, N. P., "Sampling and Measuring for NO and NO_2 in Combustion Systems," Fourteenth Aerospace Sciences Meeting, Paper 76-139, Washington, D.C., 1976.

20. Kramlick, J. C., and P. C. Malte, "Modeling and Measurement of Sample Probe Effects on Pollutant Gases Drawn from Flame Zones," Combustion Science and Technology, Vol. 18, 1978.

21. Malte, P. C., and Kramlick, J. C., "Further Observations of the Effect of Sample Probes on Pollutant Gases Drawn from Flame Zones," Combustion Science and Technology, Vol. 23, 1980.

22. Hori M., "Effects of Probing Conditions on NO_2/NO_x Ratios," Combustion Science and Technology, Vol. 23, 1980.

23. Newhall, H. K., and E. S. Starkman, "Direct Spectroscopic Determination of Nitric Oxide in Reciprocating Engine Cylinders," Society of Automotive Engineers, Paper 670122, New York, N.Y.

24. Shahed, S. M., "The Kinetics of Nitric Oxide Formation in High Pressure Combustion Processes," Ph.D. Thesis, University of Wisconsin -Madison, 1970.

25. Johnson, G. M., M. Y. Smith, and M. F. R. Mulcahy, "The Presence of NO_2 in Premixed Flames," Seventeenth Symposium (International) on Combustion, The Combustion Institute, Pittsburgh, PA, 1979.

26. Zabielski, M. F., L. G. Dodge, M. B. Colket, and D. J. Seery, "The Optical and Probe Measurement of NO: A Comparative Study, Eighteenth Symposium (International) on Combustion, The Combustion Institute, Pittsburgh, 1981.

27. Gaydon, A. G., and H. G. Wolfhard, "Flames: Their Structure, Radiation, and Temperature," Chapman and Hall, Fourth Edition, New York, 1979.

28. Tsuji, H., and I. Yamaoka, "The Sturcture of Counterflow Diffusion Flames in the Forward Stagnation Region of a Porous Cylinder," Twelfth Symposium (International) on Combustion, The Combustion Institute, Pittsburgh, PA, 1969.

29. Dean, J. A., and T. C. Rains, "Flame Emission and Atomic Absorption Spectroscopy," New York, 1971.

30. Herzberg, G., "Spectra of Diatomic Molecules," VNR Company, Second Edition, New York, 1950.

IX. APPENDIX

9.1 Sample Calculations for Determining NO Concentration from Optical Measurements

In order to calculate the concentration of nitric oxide along the optical path, the total per cent spectral absorption, the background per cent spectral absorption, and the spectral absorption coefficient were needed. The next example demonstrates the calculations which were used to determine the optical measurements.

The spectral energy of the lamp is recorded in volts four times for each elevation of the optical beam. The monochromator grating is set up at 214.8 nm and the spectral energy is 5.35 Volts when the optical beam is 6 mm from the above porous plate, there is no flame, and there is no NO between the porous plates. The fuel stream and NO-seeded air stream are started and the flame is ignited, giving a spectral energy of 2.80 Volts. The total per cent spectral absorption is

$$A_t = 1 - \frac{2.80}{5.35} = 47.7\%$$

The monochromator grating is set next to 213.8 nm and then to 215.8 nm, where the spectral energies are 2.7 and 3.1 Volts respectively. The average number between these two readings and the recorded spectral energy without the flame are used to derive the background per cent spectral absorption.

$$A_b = 1 - \frac{(2.7 + 3.1)}{2 \times 5.35} = 46\%$$

The total and background absorption are used in conjunction with the spectral absorption coefficient and relation 4.8 to obtain the NO concentration. The spectral absorption coefficient is corrected due to the depopulation of the ground vibrational state at flame temperatures, according to the Maxwell-Boltzmann distribution law (30). The ratio of the number of molecules in the first to that in the zeroth vibrational state is given by

$$\frac{N_1}{N_o} = e^{-\frac{\Delta E}{KT}}$$

where

ΔE = the difference between the two vibrational energy levels (1875 cm^{-1})

K = Boltzmann's constant (0.6952 K cm^{-1})

T = absolute temperature (K)

For the present example the temperature is 1248 K and a depopulation of 12% is calculated. Since the spectral absorption coefficent is given in Fig. 28 as a function of NO concentration, a trial and error procedure is used to get the nitric oxide concentration, which is 81 ppm for this example.

9.2 Experimental Data from Calibration Procedures and In-Situ Measurements of Nitric Oxide

Table I demonstrates the spectral energy in volts as a function of nitric oxide concentration and wavelength with a bandpass of 0.16 nm,

while table II shows again the spectral energy in Volts, but this time as a function of the monochromator slit width and wavelength with the constant nitric oxide concentration of 124 ppm as a parameter.

The spectral energy is recorded in Tables III and IV for the opposed jet burner as a function of the distance between the two porous plates for three different wavelengths with a bandpass of 0.16 nm for the cases of undoped air and air doped with 1200 ppm CH_4.

TABLE I. Spectral Energy in Volts from Calibration Results for a Bandpass of 0.16 nm

Wavelength (nm)	Nitric Oxide Concentration (ppm)							
	0	56	115	124	190	218	265	515
210.0	7.71	7.70	7.72	7.72	7.74	7.72	7.73	7.72
214.5	8.16	8.08	8.06	8.02	7.91	7.92	7.83	7.11
214.8	8.18	8.00	7.34	7.26	6.81	6.45	6.10	4.13
215.1	8.19	8.19	8.15	8.12	7.96	7.94	7.88	7.15
220.0	8.63	8.67	8.67	8.64	8.67	8.62	8.65	8.64
225.0	9.10	9.06	9.07	9.10	9.10	9.08	9.10	9.09
225.8	9.24	9.22	9.21	9.09	9.02	8.96	8.79	8.66
226.2	9.31	9.23	8.83	8.78	8.48	8.21	7.92	6.38
226.6	9.34	9.26	9.24	9.15	9.06	9.08	8.96	8.77
228.0	9.51	9.42	9.41	9.38	9.44	9.36	9.42	9.41

TABLE II. Spectral Energy in Volts from Calibration Results for a Constant NO Concentration of 124 ppm

Wavelength (nm)	Monochromator Slit Width (mm)							
	0.020	0.050	0.100	0.150	0.200	0.250	0.300	0.400
210.0	0.20	1.78	7.72	17.54	32.68	46.2	53.7	57.1
214.5	0.21	1.85	8.02	18.15	32.75	46.7	54.1	57.1
214.8	0.18	1.64	7.26	16.95	31.15	45.1	52.6	56.9
215.1	0.21	1.89	8.12	18.88	33.62	47.5	54.3	57.2
220.0	0.22	2.00	8.64	19.59	34.30	48.8	55.0	57.3

TABLE III. Spectral Energy from Experimental Runs Which Determine the NO Concentration for the Undoped Case

Distance Below Upper Porous Plate (mm)	Wavelength (nm)		
	214.0	214.8	215.6
1	1.08	1.08	1.08
2	1.17	1.16	1.18
3	1.90	1.89	1.91
4	2.48	2.41	2.49
5	2.82	2.70	2.82
6	2.88	2.80	2.89
7	2.94	2.84	2.94
8	2.96	2.86	2.97
9	2.99	2.85	3.01
10	3.76	3.57	3.77
11	4.48	4.25	4.49
12	4.66	4.43	4.68
13	3.90	3.70	3.91
14	2.24	2.12	2.24

TABLE IV. Spectral Energy from Experimental Runs Which Determine the NO Concentration for the CH_4-Doped Case

Distance Below Upper Porous Plate (nm)	Wavelength (nm)		
	214.0	214.8	215.6
1	1.08	1.08	1.09
2	1.17	1.17	1.17
3	1.90	1.90	1.92
4	2.48	2.47	2.48
5	2.82	2.79	2.83
6	2.88	2.84	2.89
7	2.94	2.86	2.95
8	2.96	2.86	2.97
9	2.99	2.85	3.00
10	3.76	3.57	3.77
11	4.48	4.25	4.49
12	4.66	4.43	4.69
13	3.90	3.70	3.91
14	2.24	2.12	2.24

The vita has been removed from the scanned document

SPECTROSCOPIC MEASUREMENT OF NITRIC OXIDE IN A DIFFUSION FLAME

by

Dimitris Valougeorgis

(ABSTRACT)

Conventional measurements of NO and NO_2 produced by a diffusion flame around a cotton ball wetted by heptane have been performed and prove that NO is oxidized to NO_2 on a mole for mole basis when the air of the flame is doped with hydrogen and that the NO to NO_2 mechanism does not require carbon atoms in the dopant.

In-situ spectroscopic measurements of NO in a laminar H_2-air diffusion flame were performed and compared to data obtained with probe sampling procedures. Ultraviolet absorption of the (1,0) gamma bands of nitric oxide near 214.8 nm were used for the spectroscopy. Spectroscopic measurements were possible only when the air stream was seeded with ca. 100 ppm NO. A conventional sampling system was operated at a probe pressure of 0.3 atmosphere and was used to sample from both the high temperature combustion zone and relatively cool regions on both sides of the flame. Spectroscopic and probe measurements of NO agree to within 30%, with probe concentrations being greater. The air of the flame was doped to give 1200 ppm methane and the NO concentrations were measured again, using probe and spectroscopic techniques. Both techniques confirm that even small unburned hydrocarbon concentrations cause the disappearance of NO on the air side of the visible reaction zone.